CHAPTER IV
RESULTS AND DISCUSSION

4.1 Screening the inert component

As solution contains n-hexane as a solvent and 7 wt% of dodecane as a tracer, justification must be made to verify whether n-hexane affects the adsorption experiments. For that purpose, Everett equation was employed, Equation (4.1) (Everett, 1964):

$$\frac{x_1' x_2'}{M_t \Delta x_1} = \frac{1}{n_m(\alpha - 1)} + \frac{1}{n_m} x_1' \qquad (4.1)$$

x_1' is molar fraction of component "1" in liquid phase
x_2' is molar fraction of component "2" in liquid phase
M_t is the initial total moles in the solution
n_m is the adsorption capacity for x_1, mol/g of adsorbent
α is the selectivity factor for x_1 relative to x_2

$x_1' x_2' / M_t \Delta x_1$ was plotted against x_1 to get a straight line. α was calculated from the equality of $n_m = 1/S$ and $\alpha = 1 + S/I$, where S stands for slope and I stands for intercept. If the intercept is zero for one component, *m*-CNB or *p*-CNB, (x_1) in the case of two component feed, the other component, n-hexane, (x_2) can be attested not to be adsorbed in the adsorbent. Therefore, the component (x_2) can be used as the inert component for the process of the adsorption.

From Figure 4.1, the straight lines from the Everett equations can be plotted for *m*-CNB and *p*-CNB, respectively. As seen from the figure, the intercepts of both lines are at zero. The selectivity factor (α) is infinity based on a simple calculation from Equation (4.1), confirming that hexane is not adsorbed in the zeolite adsorbent under the tested conditions. Hence, n-hexane can be considered to be a diluent as it has no influence on the adsorption of CNBs.

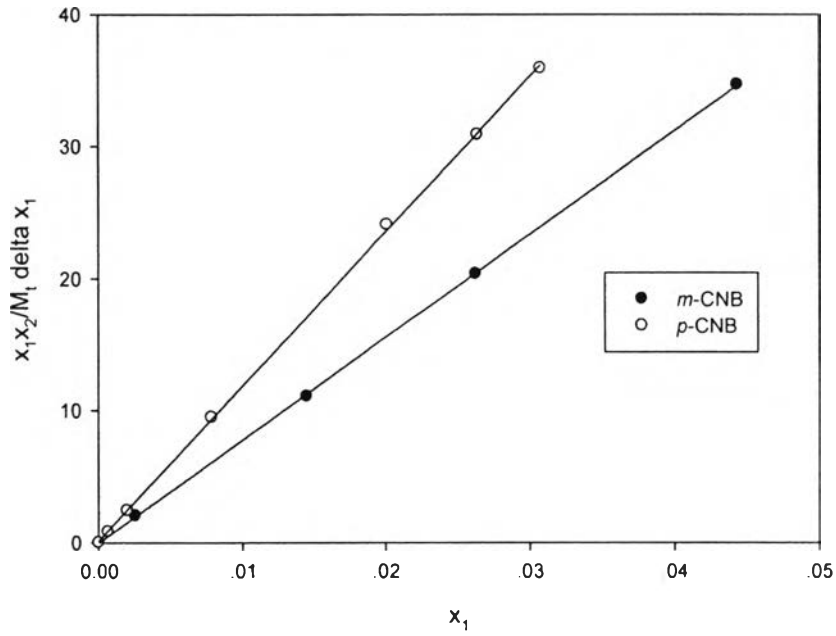

Figure 4.1 Plots of Everette equations for *m*-CNB and *p*-CNB adsorption on CsY zeolite.

4.2 Effect of X, Y zeolites, and ion exchanged on adsorption capacity

4.2.1 Single component adsorption

Single component adsorption isotherms for *m*-CNB and *p*-CNB on various zeolites obtained at 30°C are shown in Figures 4.2 to 4.21. The adsorption capacities of *m*-CNB and *p*-CNB increase at the low concentration of *m*-CNB and *p*-CNB and reach the plateau region at high concentration. With the increase in the adsorption amount, the affinity between the adsorbate and the adsorbent decreases resulted from the shield against the adsorption sites (Liu *et al.*, 2007). All adsorbents show the same trend of the isotherm. The adsorption isotherms are usually described by the classical Langmuir model. The Langmuir model, Equation (4.2), is used to fit with the experimental data. The equilibrium adsorption capacity (Q) is expressed in grams of adsorbed component on zeolite per gram of adsorbent.

$$Q = \frac{Q_{max} K C_e}{1 + K C_e}, \tag{4.2}$$

where C_e refers to the equilibrium concentration, Q_{max} is the maximum capacity or saturation capacity, and K is the equilibrium constant.

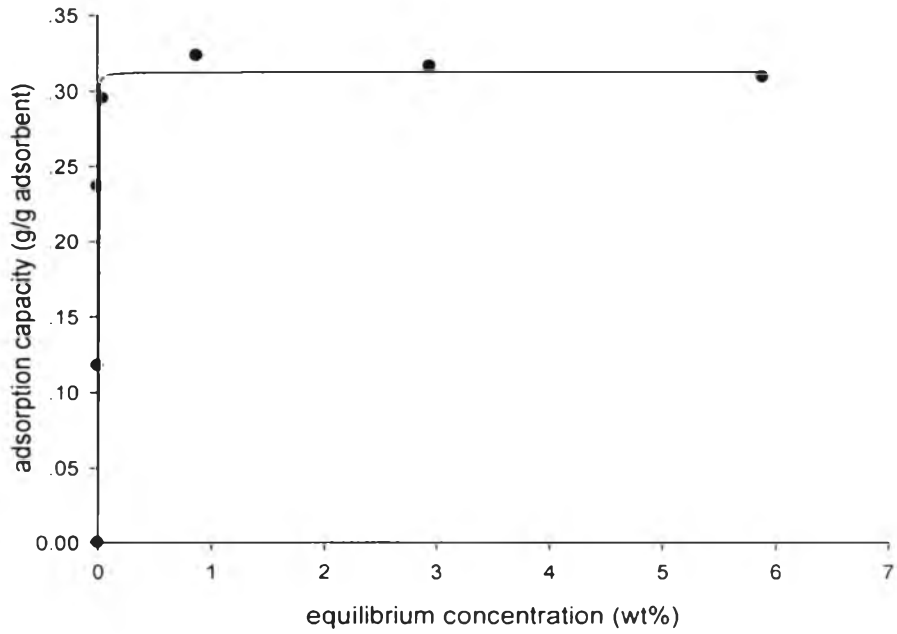

Figure 4.2 Adsorption isotherm for *m*-CNB on LiY zeolite at 30°C.

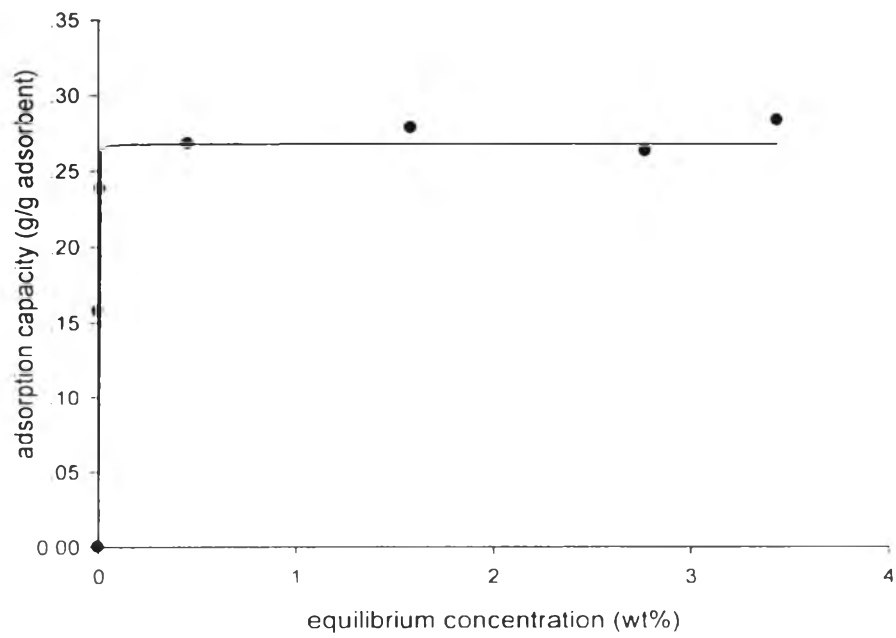

Figure 4.3 Adsorption isotherm for *p*-CNB on LiY zeolite at 30°C.

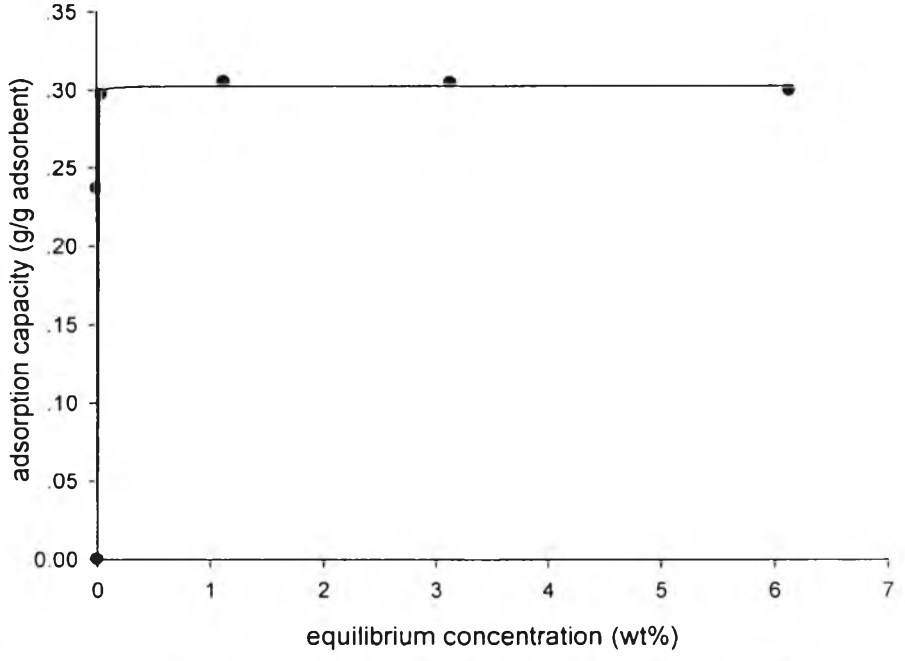

Figure 4.4 Adsorption isotherm for *m*-CNB on NaY zeolite at 30°C.

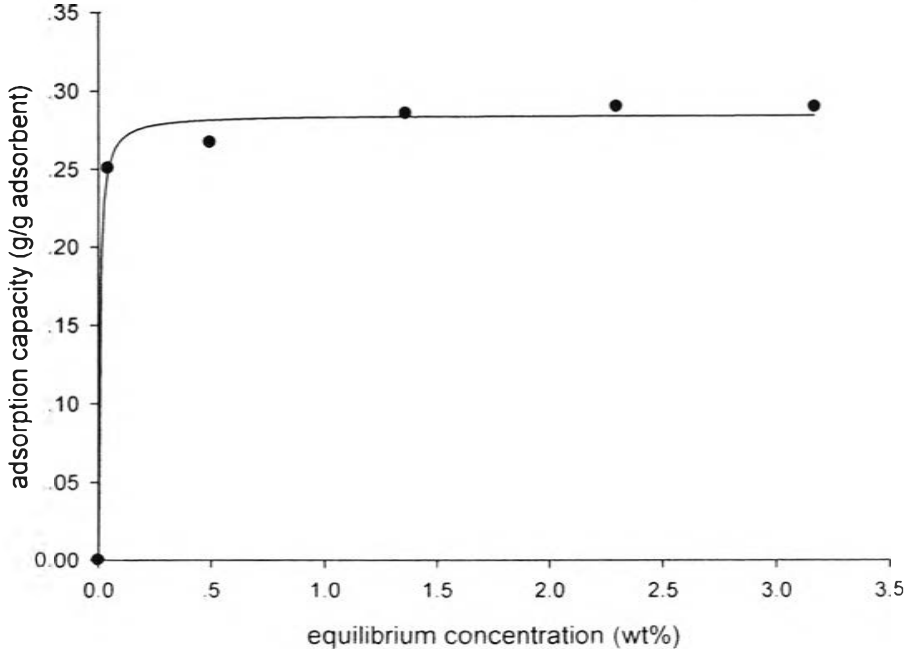

Figure 4.5 Adsorption isotherm for *p*-CNB on NaY zeolite at 30°C.

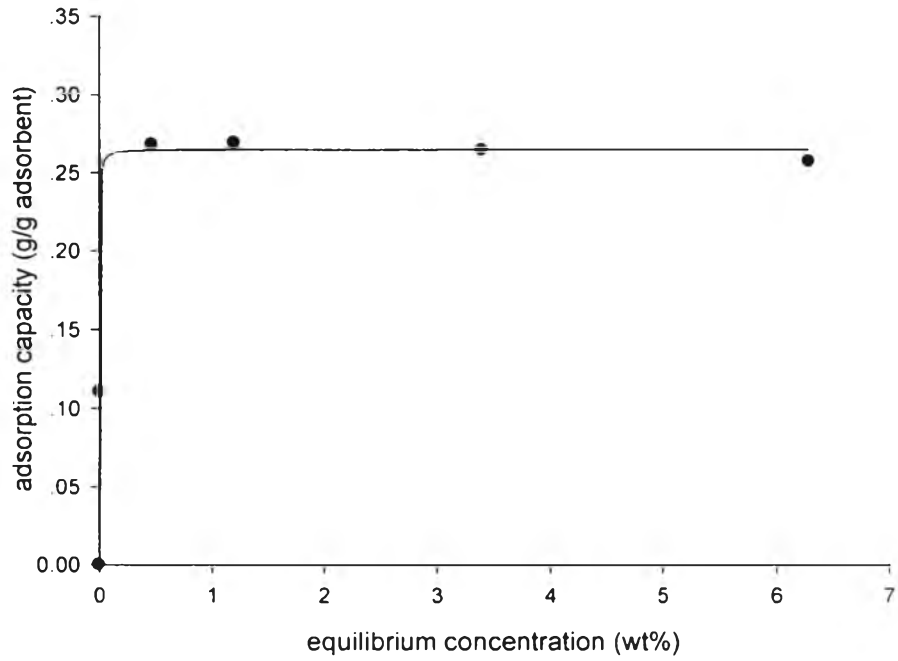

Figure 4.6 Adsorption isotherm for *m*-CNB on KY zeolite at 30°C.

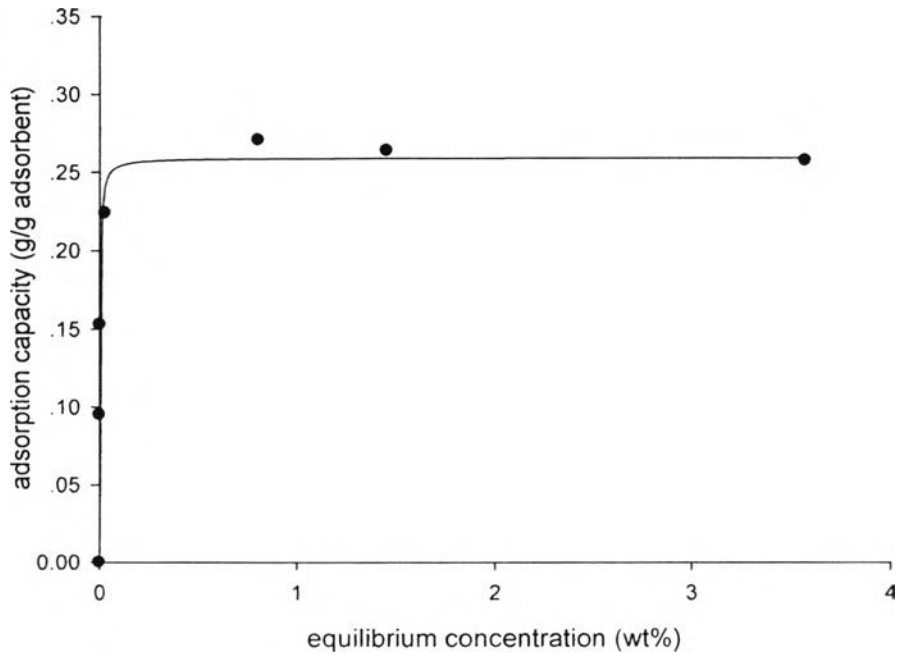

Figure 4.7 Adsorption isotherm for *p*-CNB on KY zeolite at 30°C.

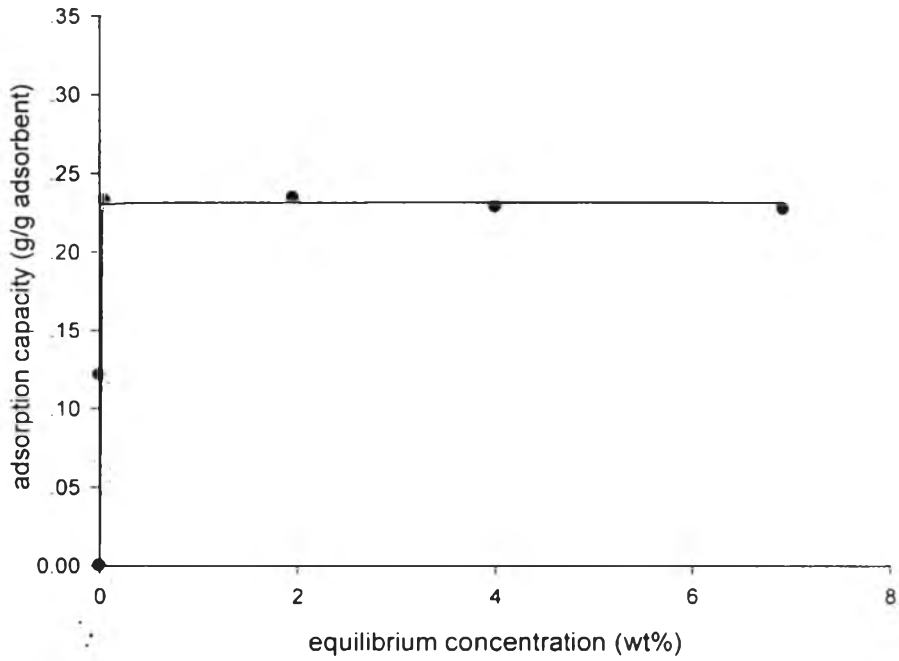

Figure 4.8 Adsorption isotherm for *m*-CNB on RbY zeolite at 30°C.

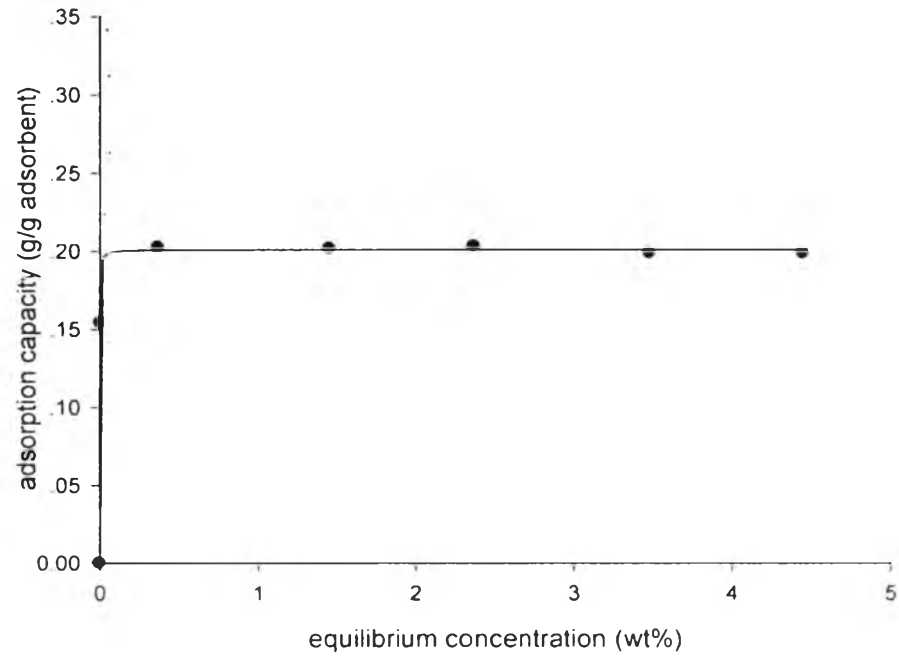

Figure 4.9 Adsorption isotherm for *p*-CNB on RbY zeolite at 30°C.

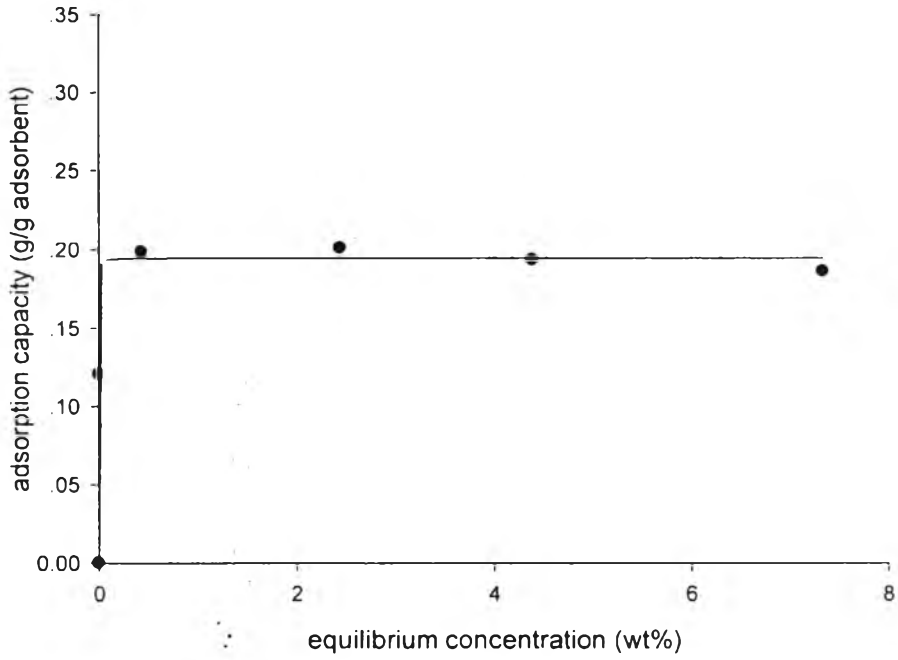

Figure 4.10 Adsorption isotherm for *m*-CNB on CsY zeolite at 30°C.

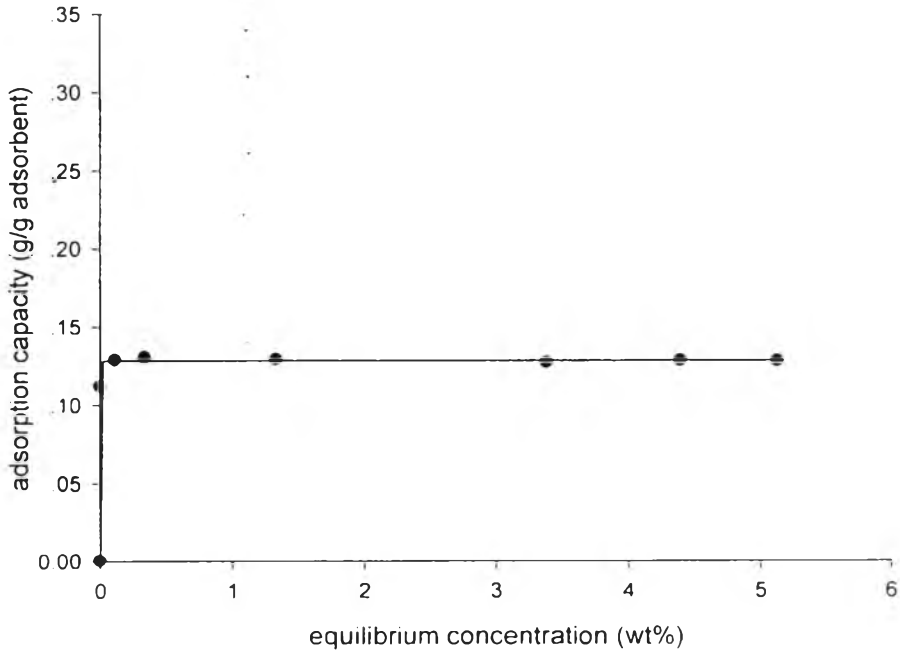

Figure 4.11 Adsorption isotherm for *p*-CNB on CsY zeolite at 30°C.

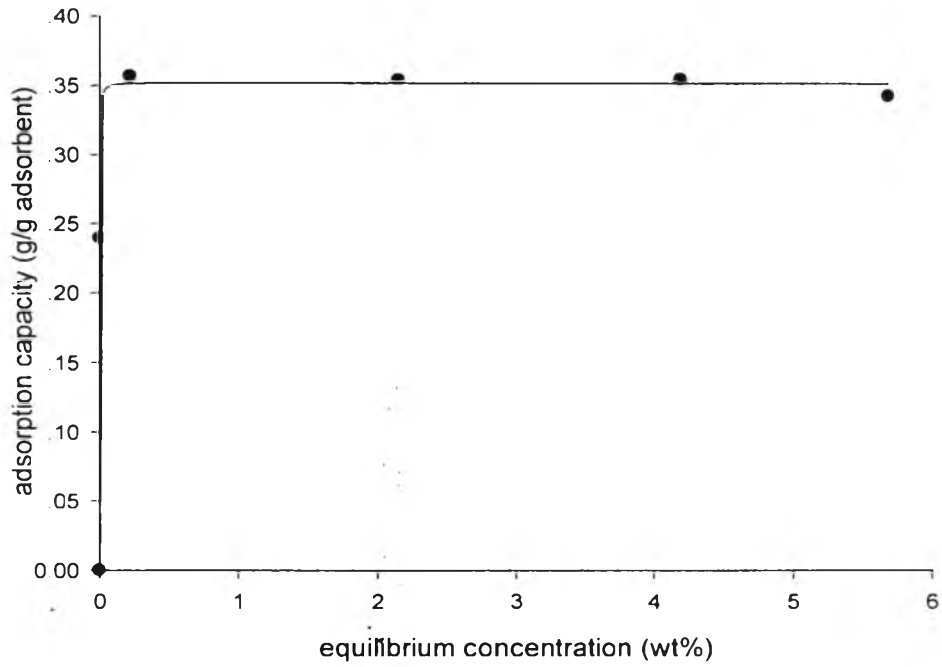

Figure 4.12 Adsorption isotherm for *m*-CNB on LiX zeolite at 30°C.

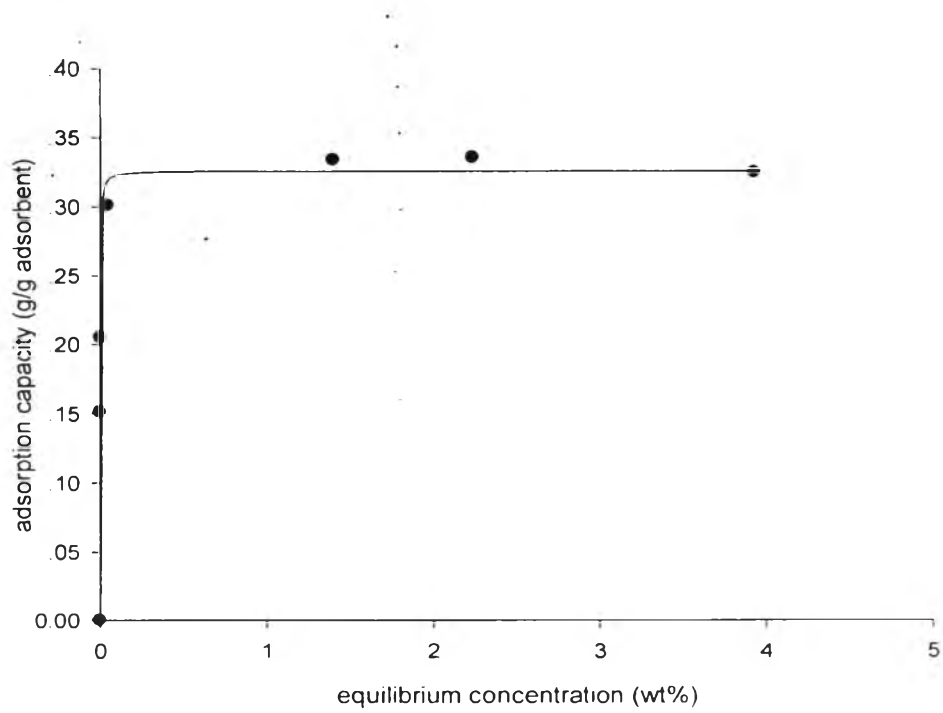

Figure 4.13 Adsorption isotherm for *p*-CNB on LiX zeolite at 30°C.

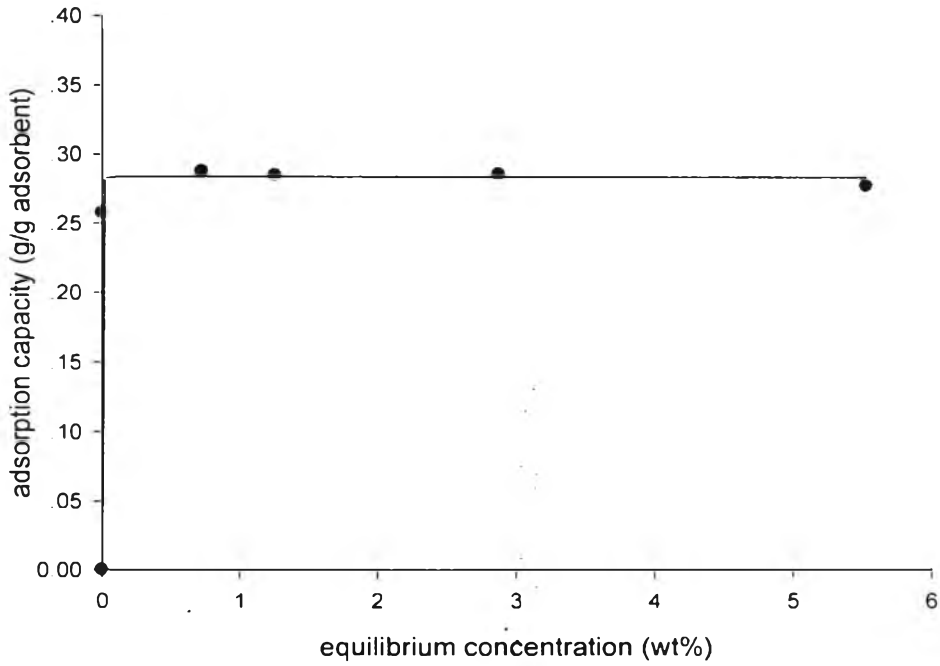

Figure 4.14 Adsorption isotherm for *m*-CNB on NaX zeolite at 30°C.

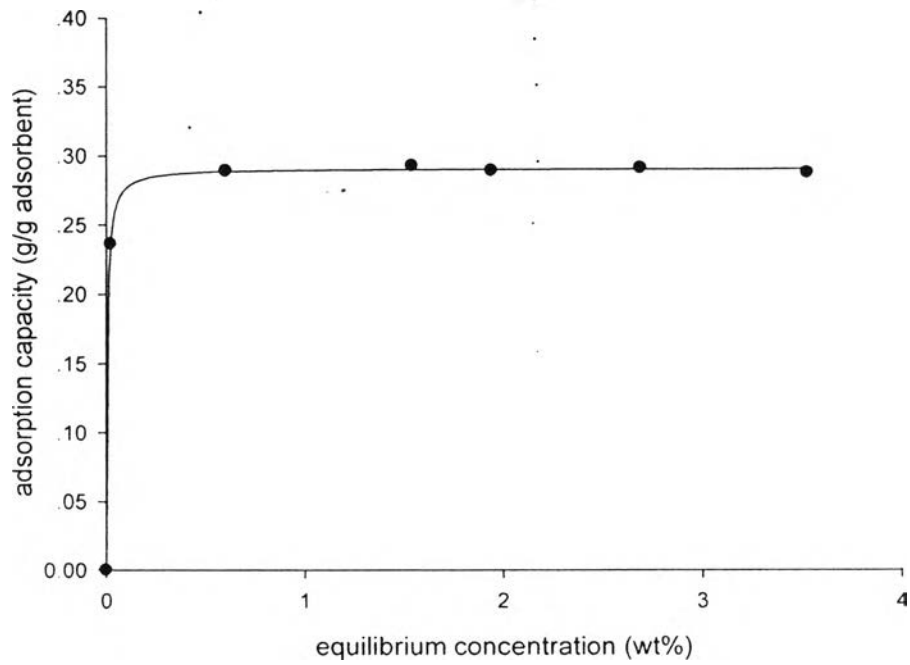

Figure 4.15 Adsorption isotherm for *p*-CNB on NaX zeolite at 30°C.

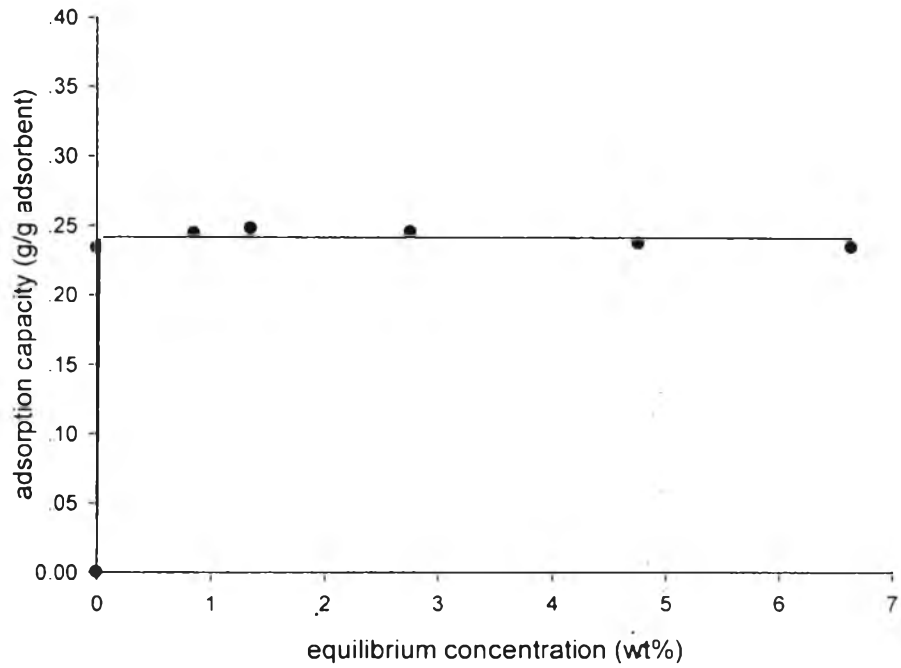

Figure 4.16 Adsorption isotherm for *m*-CNB on KX zeolite at 30°C.

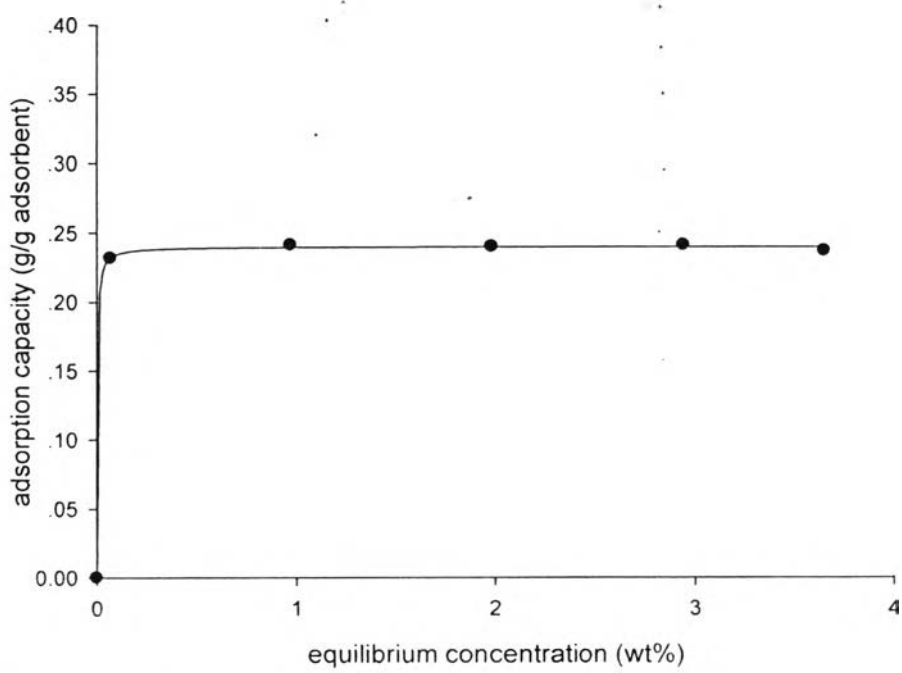

Figure 4.17 Adsorption isotherm for *p*-CNB on KX zeolite at 30°C.

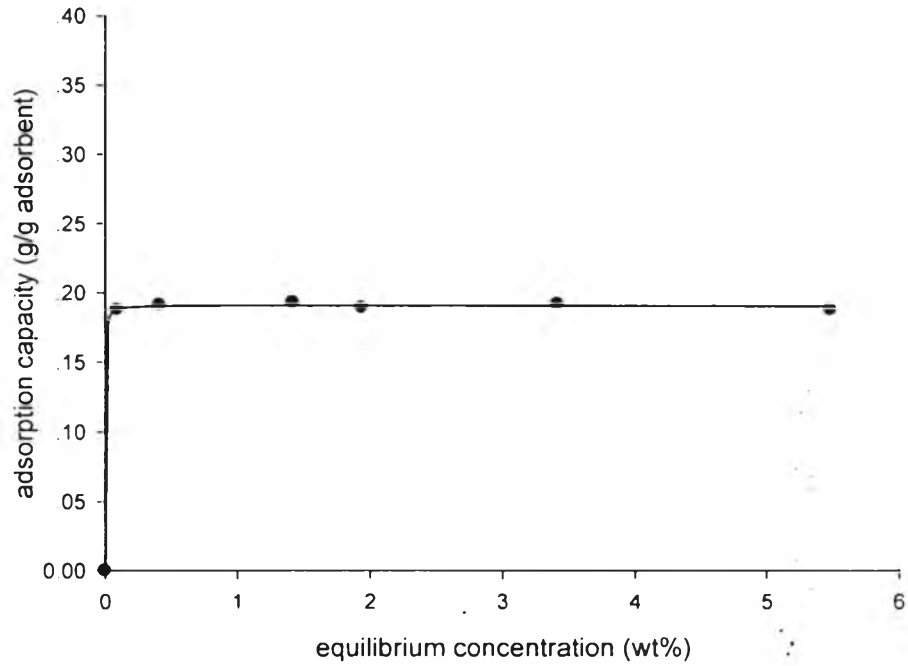

Figure 4.18 Adsorption isotherm for *m*-CNB on RbX zeolite at 30°C.

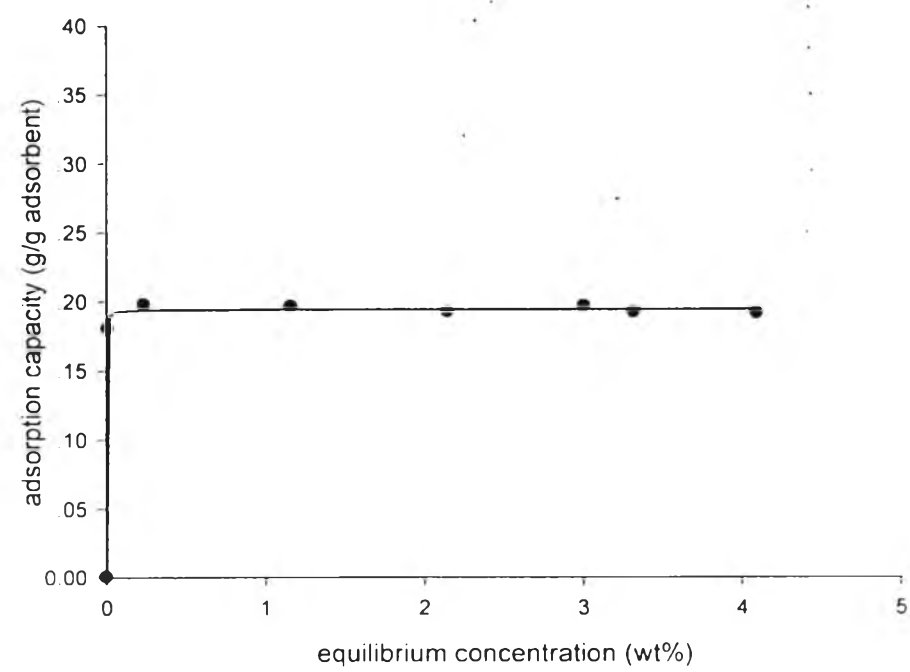

Figure 4.19 Adsorption isotherm for *p*-CNB on RbX zeolite at 30°C.

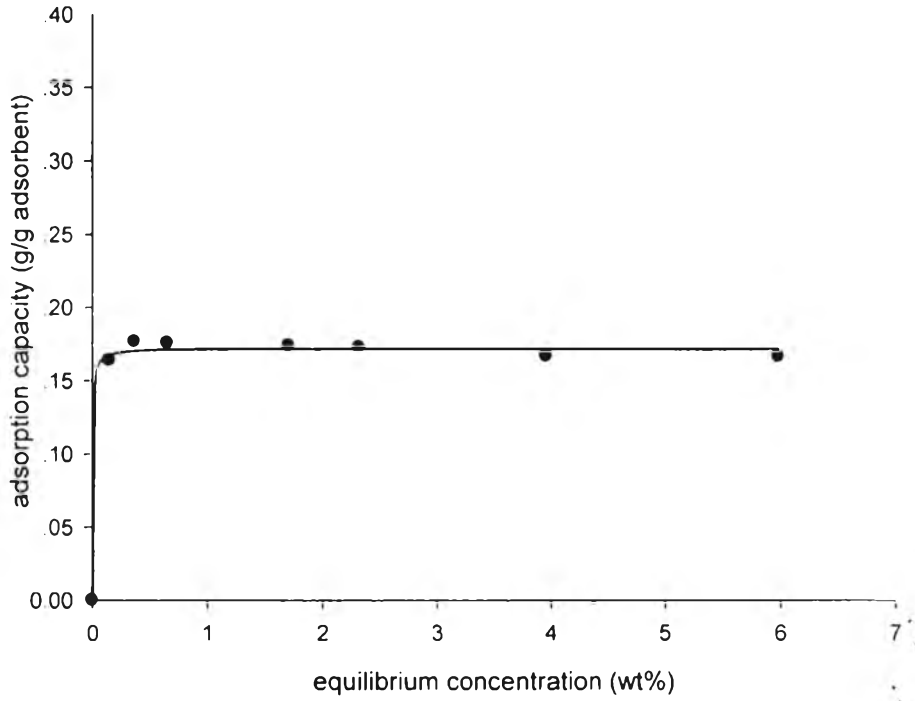

Figure 4.20 Adsorption isotherm for *m*-CNB on CsX zeolite at 30°C.

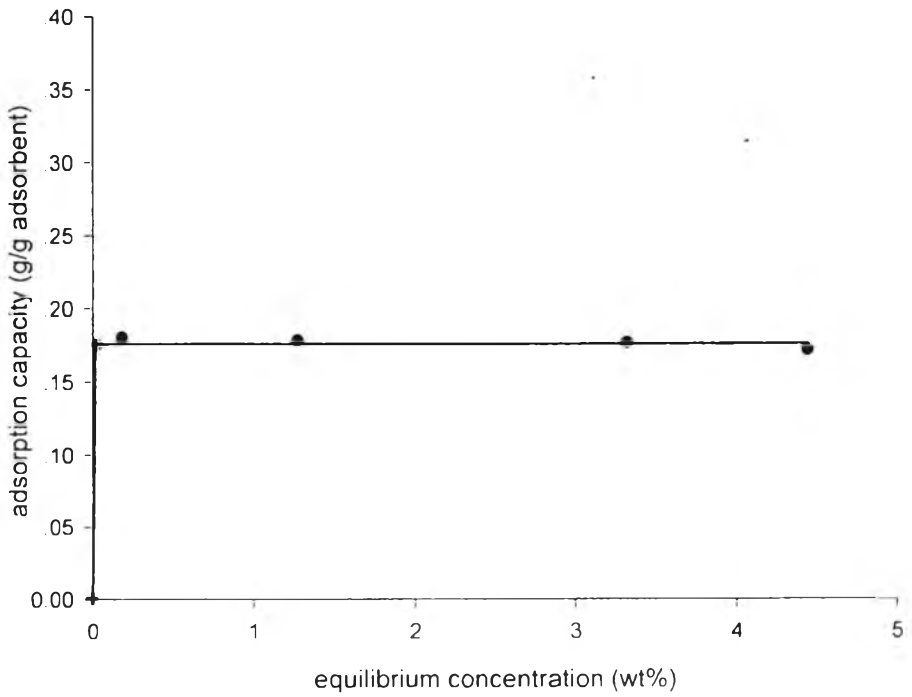

Figure 4.21 Adsorption isotherm for *p*-CNB on CsX zeolite at 30°C.

The estimated values of the adjustable parameters of the isotherms, which are maximum capacity, equilibrium constant, and the coefficient of determination, R^2, are reported in Table B2. The R^2 values close to one indicate that the equation is a good description of the relation between the independent and dependent variables. The Langmuir model is fitted well with all experimental data.

Table 4.1 Kinetic diameters and molecular dipole moments of *m*-CNB and *p*-CNB

CNB isomer	Kinetic diameter (Å)	Molecular dipole moment (D)
m-CNB	5.79	3.73
p-CNB	5.27	2.83

Adsorption capacity depends on many factors that control the adsorption mechanism. From Table 4.1 and Figure 4.22, the monovalence ion exchanged Y zeolites preferentially adsorb *m*-CNB than *p*-CNB. As the kinetic diameters of both isomers are smaller than the zeolite pores (7.4 Å) (Breck, 1974), each isomer can easily pass through the pores. It seems that the adsorption of the CNBs is not controlled by the molecular diffusion. The ¶ electrons of the aromatic ring are expected to interact with the cations on the zeolite framework leading to the Lewis acid-base interactions. Generally, bigger alkali metal cations are less acidic, which means a higher charge density borne by the oxygen atoms of the framework, leading to a decrease of interaction with aromatic molecules (Laborde-Boutet *et al.*, 2006). Not only acid-base interaction, other possible reasons that can explain the adsorption behavior may be due to the difference in molecular dipole moments (μ) and the electron density on the framework or acid-base interaction.

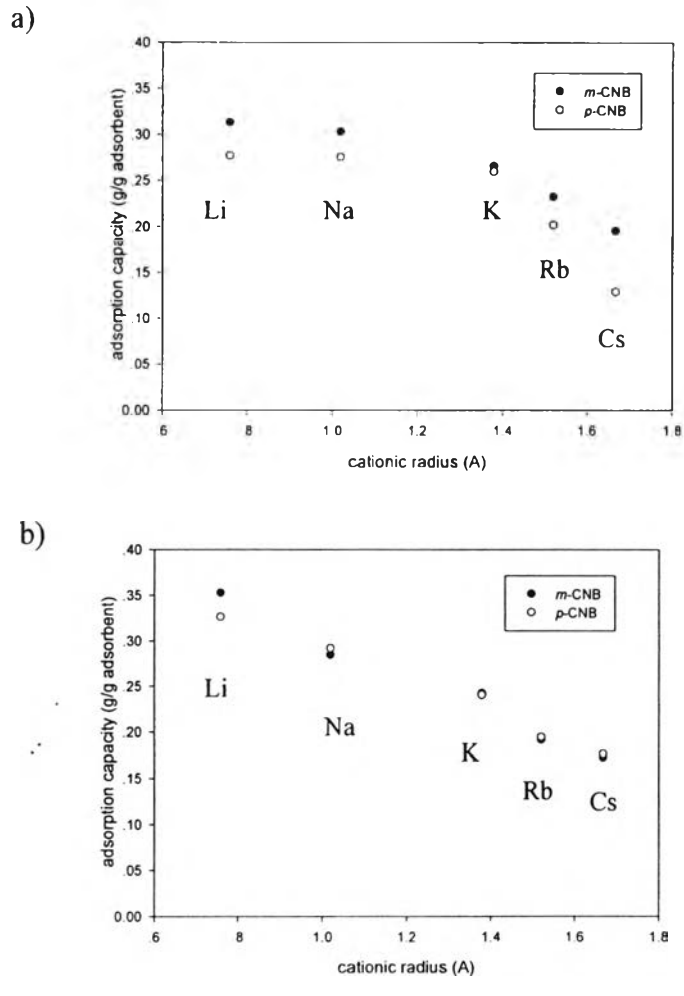

Figure 4.22 Adsorption capacity as a function of cationic radius: a) Y zeolite b) X zeolite

Higher molecular dipole moments have higher electron density around molecules and the faujasite zeolites are electron rich framework. *m*-CNB that has higher molecular dipole will adsorb on the zeolite framework more than *p*-CNB that has lower molecular dipole moment (Table 4.1). Because of its hydrophilicity and polarity, the adsorption onto X and Y zeolites mainly relies on the well-known ¶-¶ interaction (between the benzene rings of solute and adsorbate), while another interaction, the electrostatic interaction between the group of -Cl and -NO_2 on the adsorbent, is additionally introduced during the adsorption onto zeolite (Liu *et al.*, 2007).

Several works have reported that aromatics adsorption on S_{II} sites diminished in strength as the cation electropositivity increased. This phenomenon is

attributed to a lowering interaction of the aromatic ring with the cation, supposed to be less acidic. The higher Sanderson's intermediate electronegativity of the adsorbents (S_{int}, Table B2) indicates high electron accepting ability and strong adsorbent acid strength (Mortier, 1978). On the series of monovalence ion exchanged X zeolite, all zeolites have lower acid strength than Y zeolite. So, all X zeolites have comparable adsorption capacities for both components except for LiX. When Sanderson's intermediate electronegativity of zeolites is lower than that of LiX, the molecular dipole moments of both isomers seem not to affect their adsorption capacities.

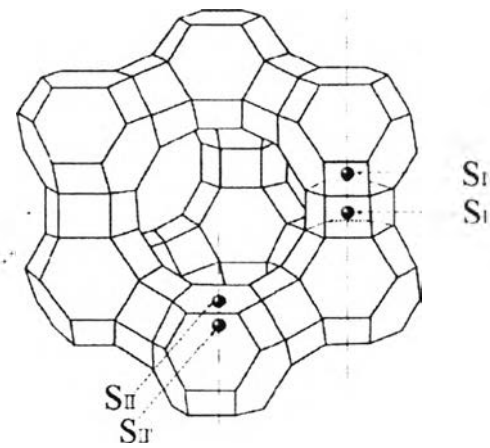

Figure 4.23 Structure and cationic sites in Y faujasites.

One should note that these ion exchanged zeolites correspond to a substitution of most of the cations located in $S_{II}/S_{II'}$ sites of the zeolite structure (Figure 4.23), which are more easily exchanged than $S_I/S_{I'}$ cations. It is enough for having significant influences upon *m*-CNB and *p*-CNB adsorption, since these sorbates can interact with S_{II} type surroundings but remain too large to enter the areas where the $S_I/S_{I'}$ cations are located (Laborde-Boutet *et al.*, 2006).

From the same series of alkaline in X and Y zeolites, it can also be observed that both adsorption capacities decrease with lower acid strength zeolites and larger cationic radius as shown in Figure 4.23. Larger cationic radius will block some adsorption sites that affect the adsorption capacities (Frising *et al.*, 2008).

4.2.2 Binary component competitive adsorption

Binary competitive adsorption isotherms for equimolar mixtures of *m*-CNB and *p*-CNB as a feed mixture on various zeolites are shown in Figures 4.24 to 4.33. For LiY, the adsorption capacities of *m*-CNB increase with the concentration of *m*-CNB, and equal 0.1648 g/g adsorbent calculated from the curve in the final stage of the competitive adsorption. However, the adsorption capacities of *p*-CNB increase faster at the initial stage up to 0.2 wt% of the concentration. After that, the adsorption capacities reach a lower asymptotic level as the concentration increases further. Because of competition between *m*-CNB and *p*-CNB on the adsorbent, the binary competitive adsorption isotherms are different from the single adsorption isotherms. The main reason is strong electrostatic field interaction between the zeolite and the isomers. Thus, the competition for the adsorption sites is considered to be the predominant mechanism. From Table 4.1, kinetic diameters of *m*-CNB and *p*-CNB indicate that they can diffuse though the zeolite pore and adsorb. But each competitive adsorption isotherm shows that *m*-CNB and *p*-CNB adsorption capacity change along equilibrium concentration. This result shows that the adsorption should not be controlled by only the molecular diffusion (rate-selective mechanism).

The adsorption isotherm of *m*-CNB is different from that of *p*-CNB for LiY, NaY, KY, LiX, NaX, and KX. Because of high acid strength zeolites, higher electrostactic fields strongly interact with *m*-CNB more than *p*-CNB. Hence, *m*-CNB adsorption capacities are higher than those of *p*-CNB. However, the trends are not the same for low acid strength zeolites and bigger cationic radius, RbX, CsX, RbY and CsY. When adsorbents have low acid strength or low electron accepting ability, both *m*-CNB and *p*-CNB adsorption capacities are not quite different, resulting in more or less the same adsorption capacities of both isomers. The above results support the idea that the adsorption capacities for both *m*-CNB and *p*-CNB may depend on the acid base interaction between the components and the electrostatic field on the zeolites.

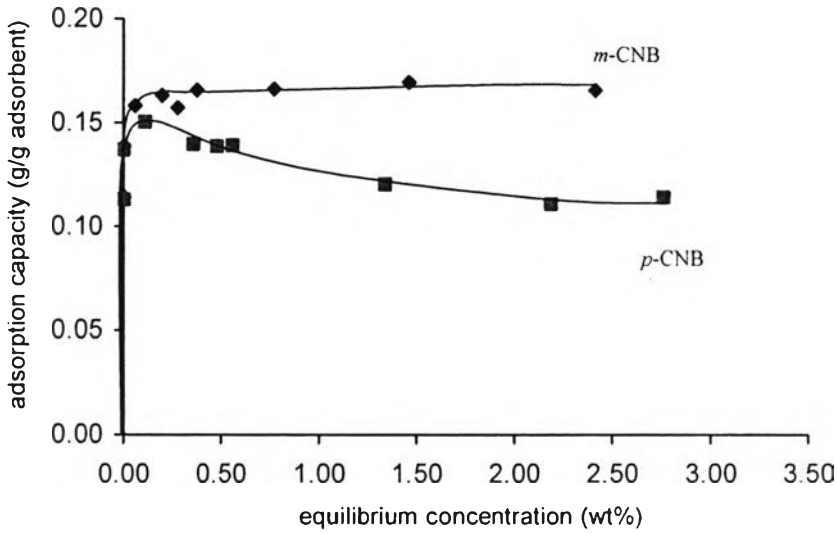

Figure 4.24 Binary adsorption isotherms for *m*-CNB/*p*-CNB on LiY zeolite at 30°C.

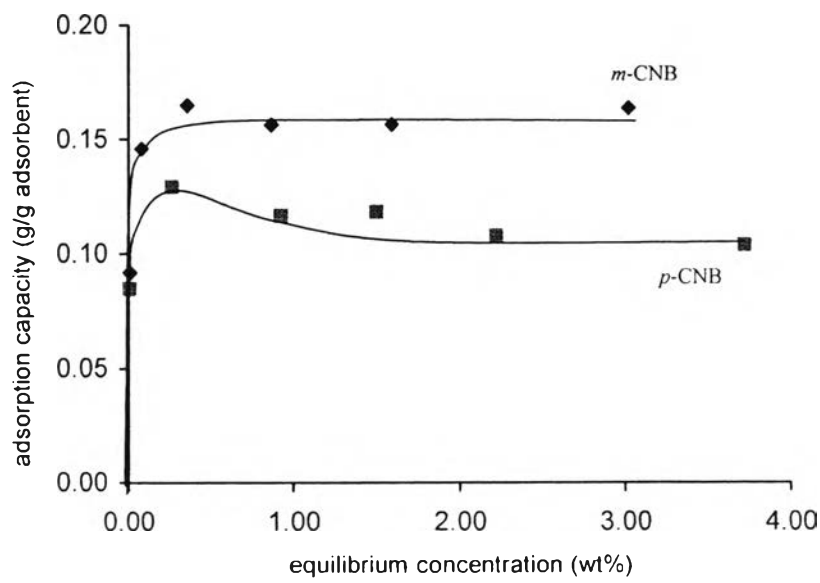

Figure 4.25 Binary adsorption isotherms for *m*-CNB/*p*-CNB on NaY zeolite at 30°C.

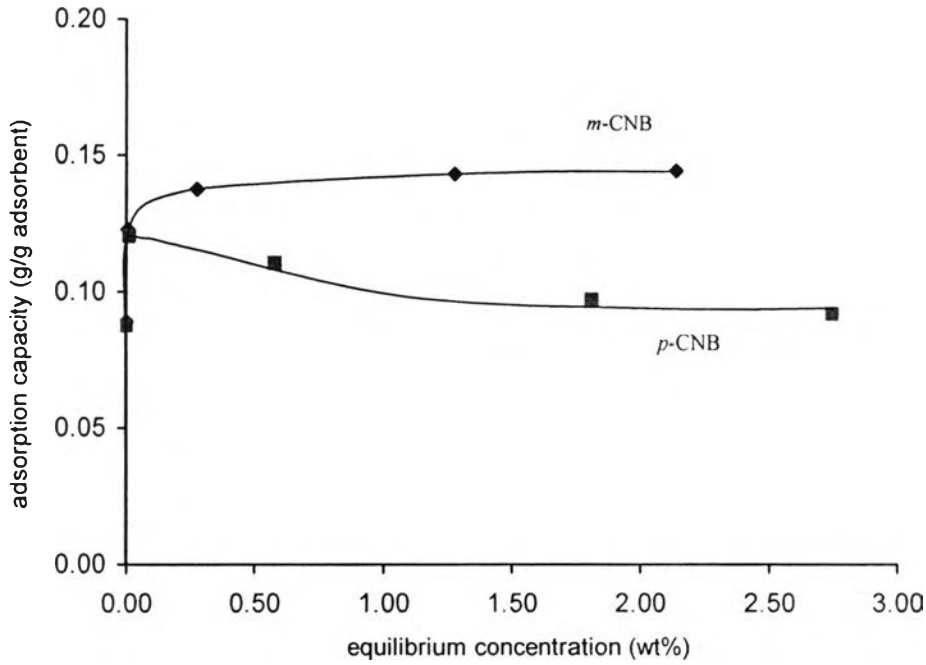

Figure 4.26 Binary adsorption isotherms for *m*-CNB/*p*-CNB on KY zeolite at 30°C.

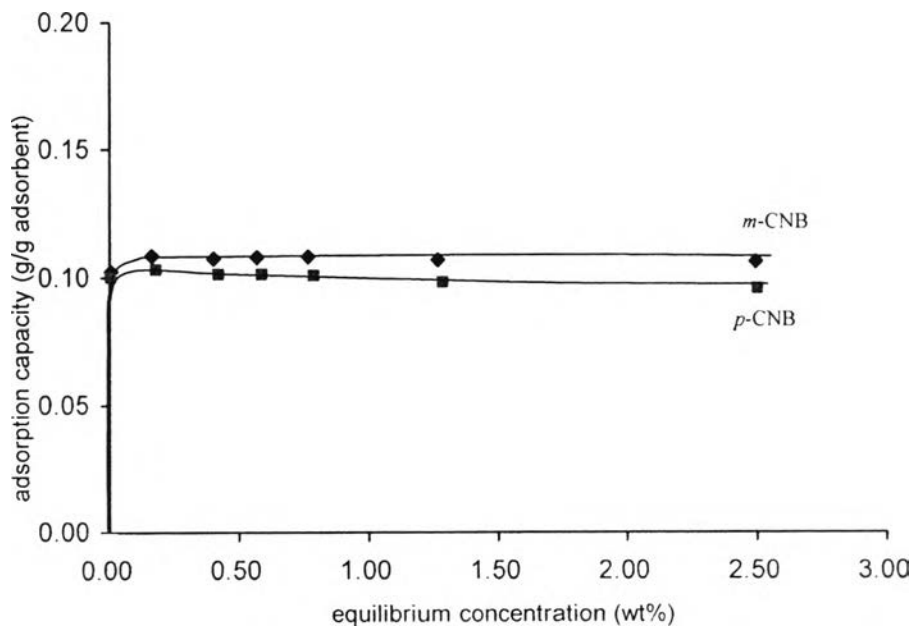

Figure 4.27 Binary adsorption isotherms for *m*-CNB/*p*-CNB on RbY zeolite at 30°C.

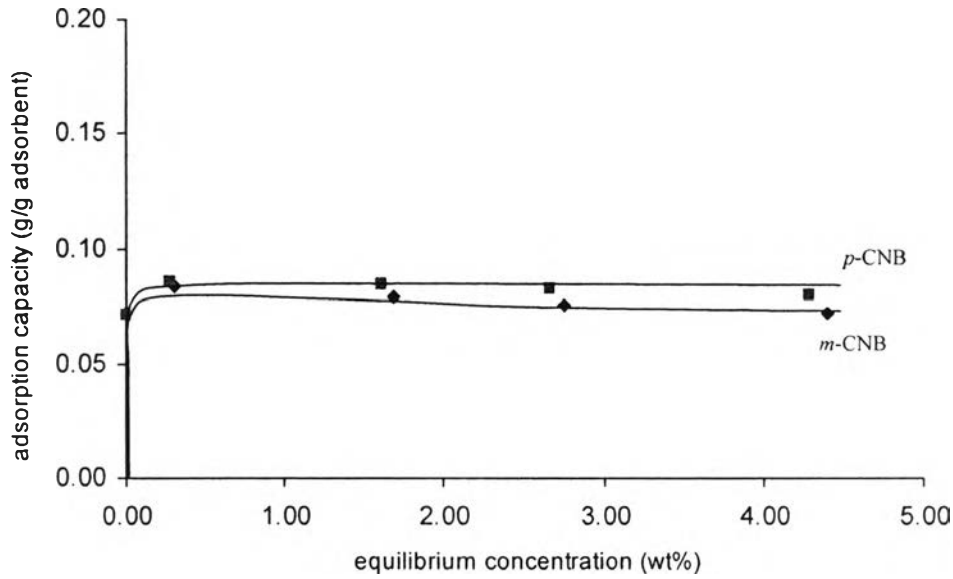

Figure 4.28 Binary adsorption isotherms for *m*-CNB/*p*-CNB on CsY zeolite at 30°C.

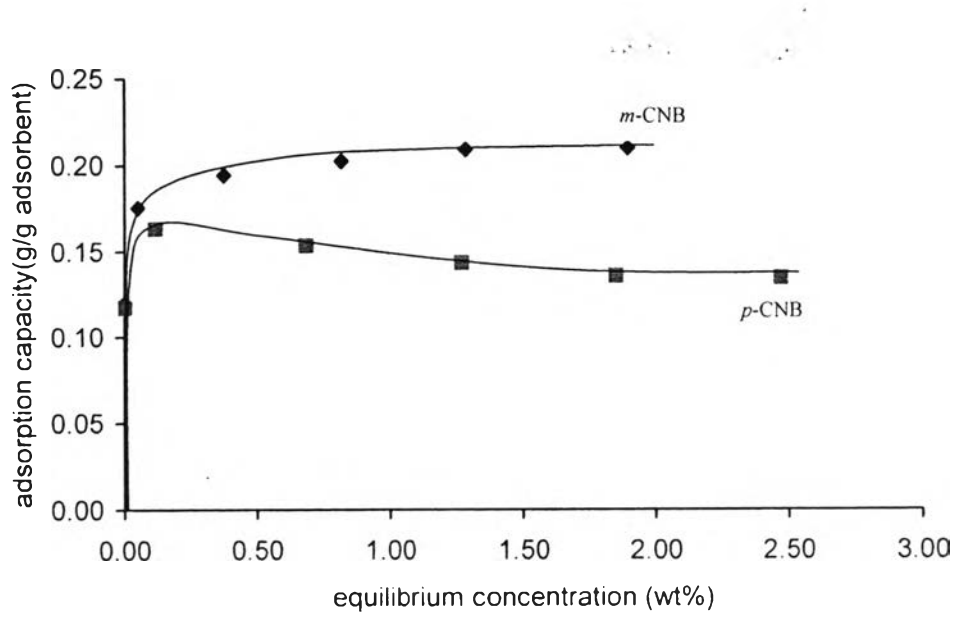

Figure 4.29 Binary adsorption isotherms for *m*-CNB/*p*-CNB on LiX zeolite at 30°C.

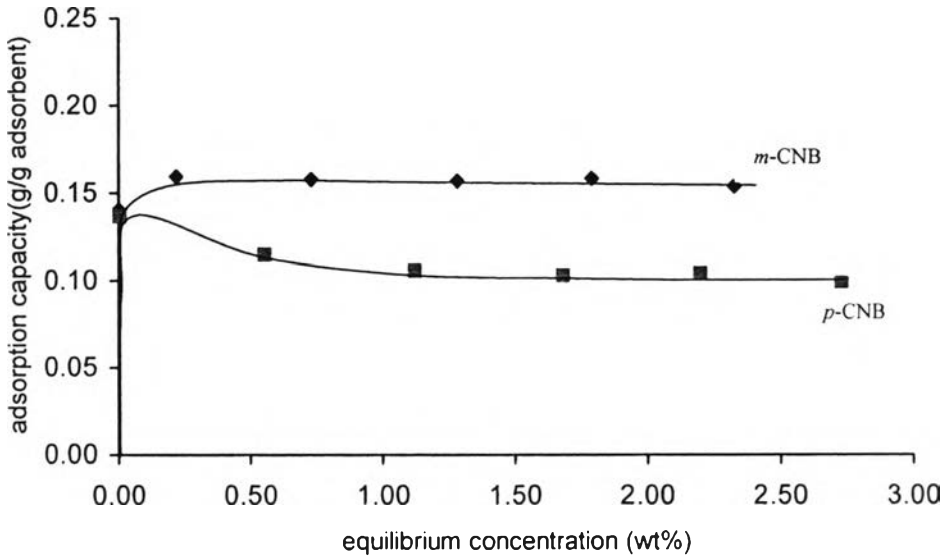

Figure 4.30 Binary adsorption isotherms for *m*-CNB/*p*-CNB on NaX zeolite at 30°C.

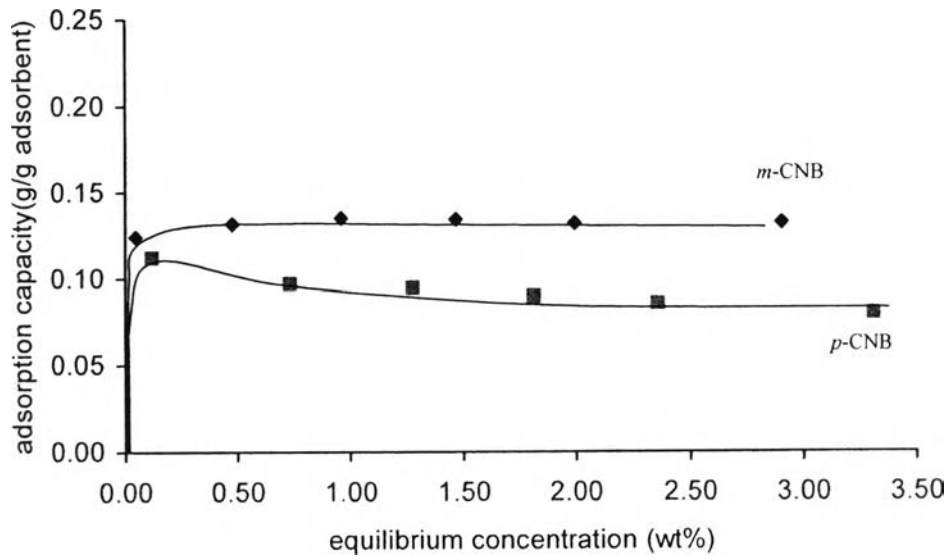

Figure 4.31 Binary adsorption isotherms for *m*-CNB/*p*-CNB on KX zeolite at 30°C.

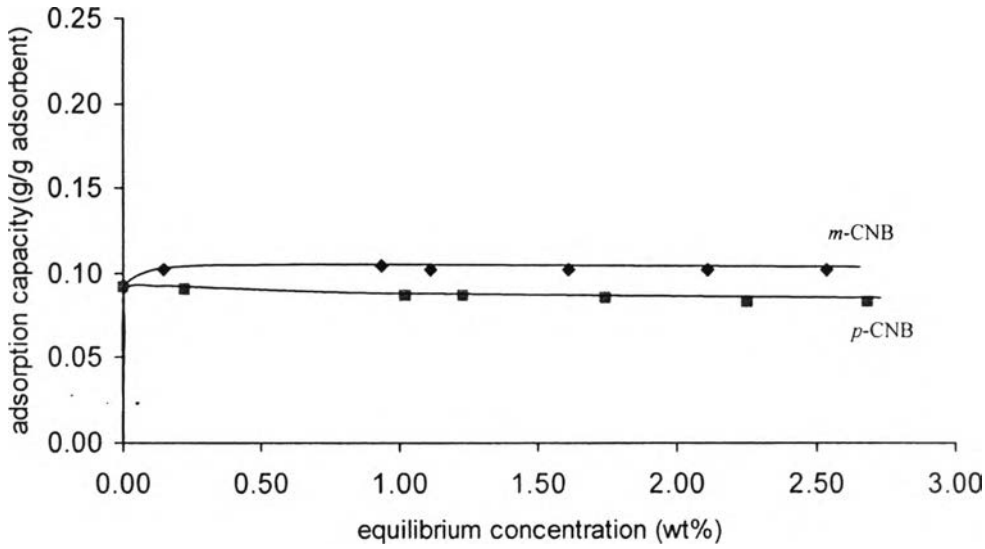

Figure 4.32 Binary adsorption isotherms for *m*-CNB/*p*-CNB on RbX zeolite at 30°C.

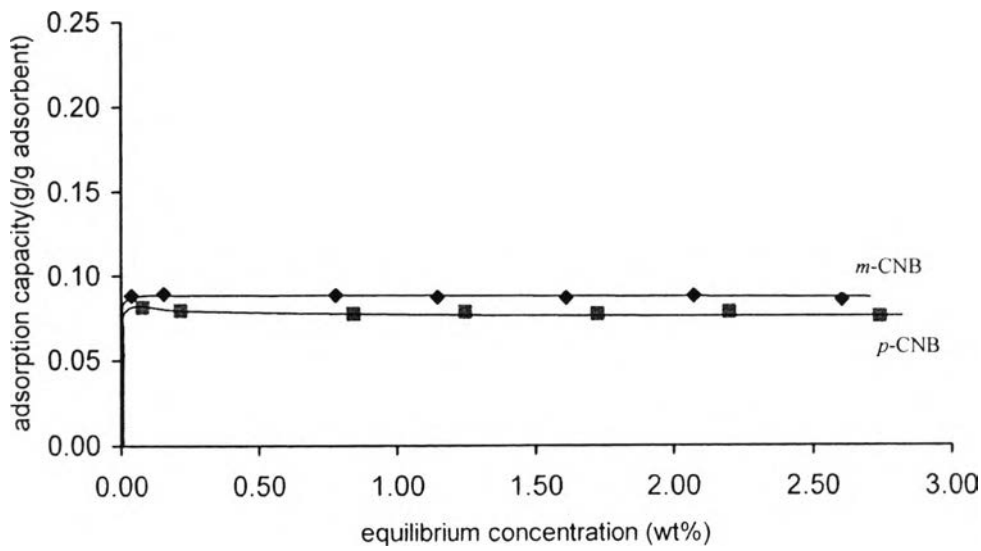

Figure 4.33 Binary adsorption isotherms for *m*-CNB/*p*-CNB on CsX zeolite at 30°C.

On the other hand, the influence of the initial concentration of *m*-CNB upon the adsorption amount of *p*-CNB is shown in Figure 4.34. *p*-CNB capacities decrease with increase in *m*-CNB initial concentration. At low concentration, there is enough space in the zeolite to receive all the species of the adsorbates. *p*-CNB ad-

sorbs higher at low initial concentration. At higher initial concentration, *p*-CNB capacities are lower due to adsorption competition between each isomer. There is a drop in the adsorption amount of *p*-CNB especially for high acid strength zeolites, LiX, LiY and NaY. However, increasing cationic radius or decreasing adsorbent acid strength, *p*-CNB capacities are almost constant with an increase in the initial concentration. Only for high acid strength zeolites, the *p*-CNB adsorption capacity depends on the *m*-CNB initial concentration.

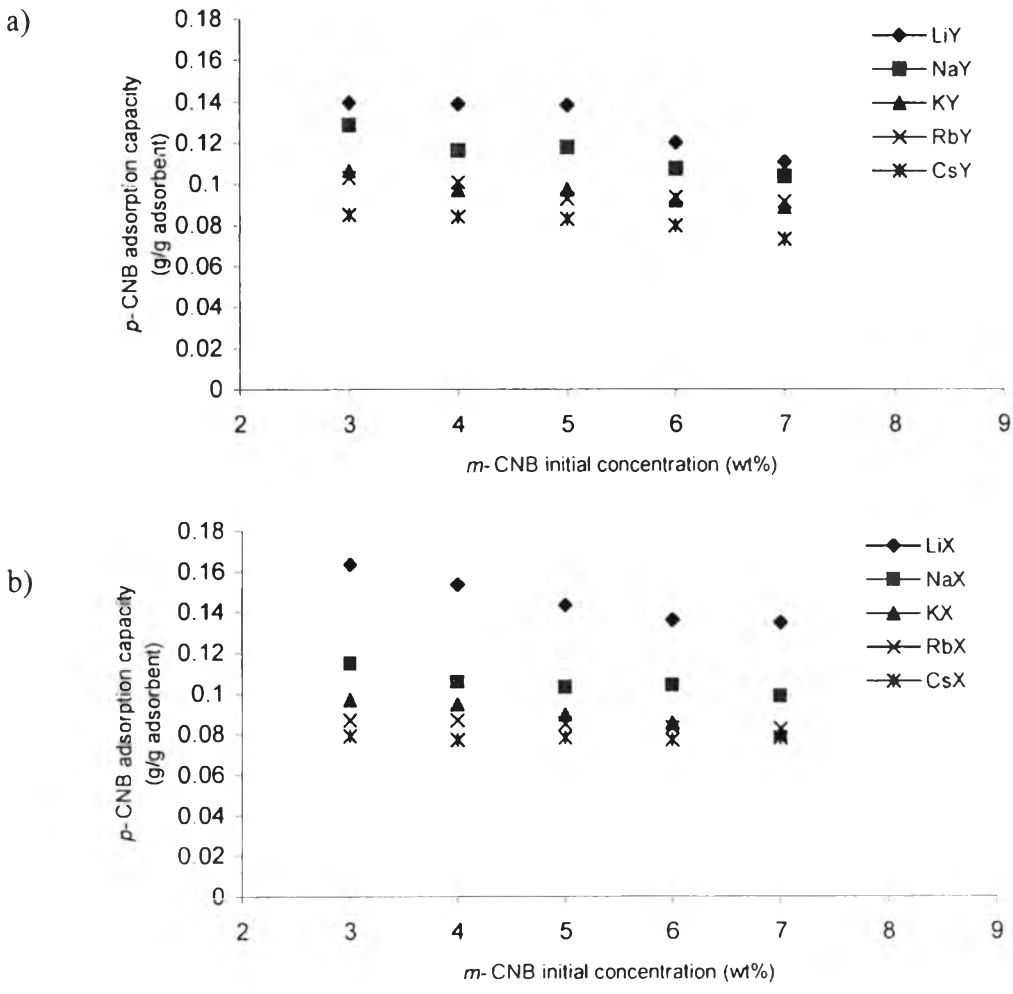

Figure 4.34 Adsorption capacities of *p*-CNB on monovalence cation exchanged (a) Y zeolites and (b) X zeolites.

On the series of ion exchanged Y zeolite, because of adsorbate-adsorbent interaction and adsorbate-adsorbate interaction, binary adsorption isotherms are not similar to those of *m*-CNB and *p*-CNB single adsorption. However, the total adsorption isotherms are the same as the Langmuir isotherm as shown in Figure 4.35. The total adsorption capacities of the zeolites for both components were obtained from the summation of individual adsorption capacities at the same initial concentration and reported in Table B1. The summation capacities for the binary system show the same trend with the single adsorption systems. All adsorbents have the same trend of adsorbent isotherms.

a)

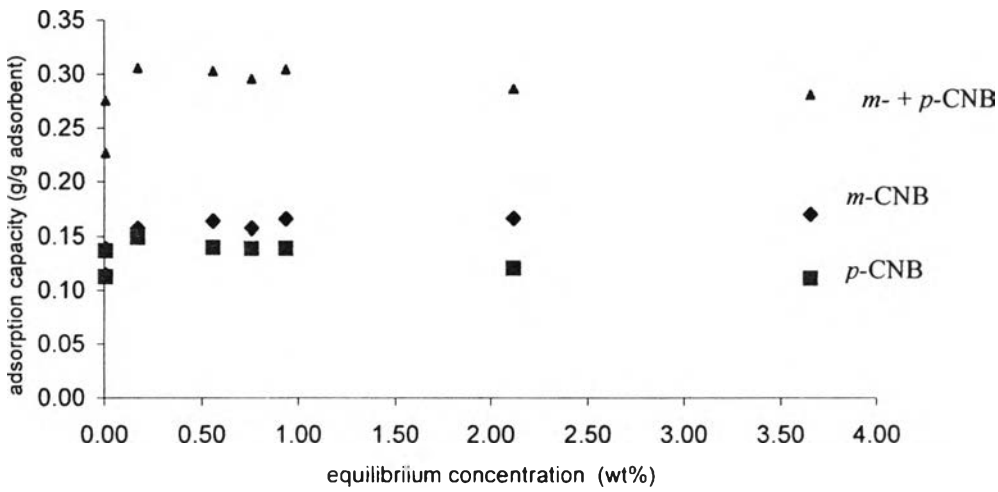

b)

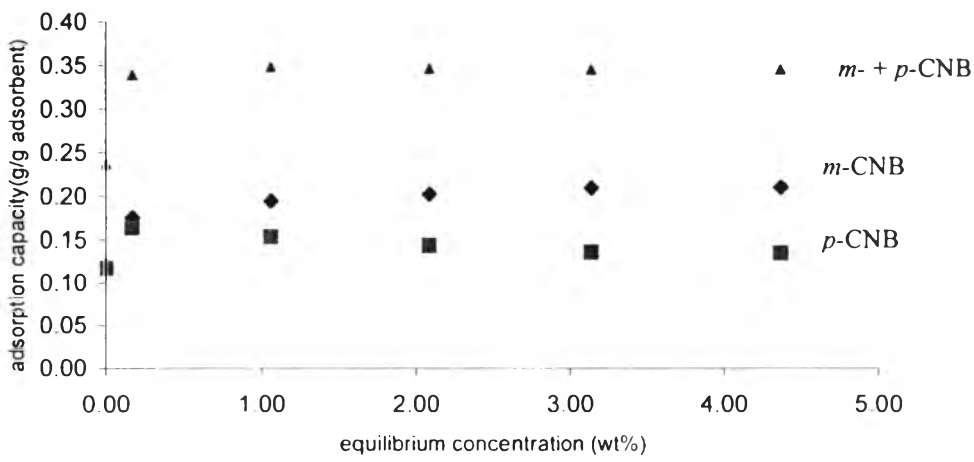

Figure 4.35 Binary competitive and total capacity adsorption isotherms at 30°C a) LiY b) LiX.

The adsorption capacity of *m*-CNB decreases as the size of the cation increases due to the decrease in the acid strength of the adsorbent with increasing the cationic size. For the para form, the adsorption capacities are relatively constant within the series of Y zeolite. Hence, the acid strength of the adsorbent does not influence a great deal of the *p*-CNB adsorption capacities as shown in Figure 4.36. Unlike the series of X zeolite, the acid strength does slightly influence on the *p*-CNB adsorption capacities. For the Y zeolites, the adsorption capacity of *m*-CNB decreases with the increase in the cationic size. The total capacity decreases for both X and Y zeolites with lower acid strength as in the single adsorption system.

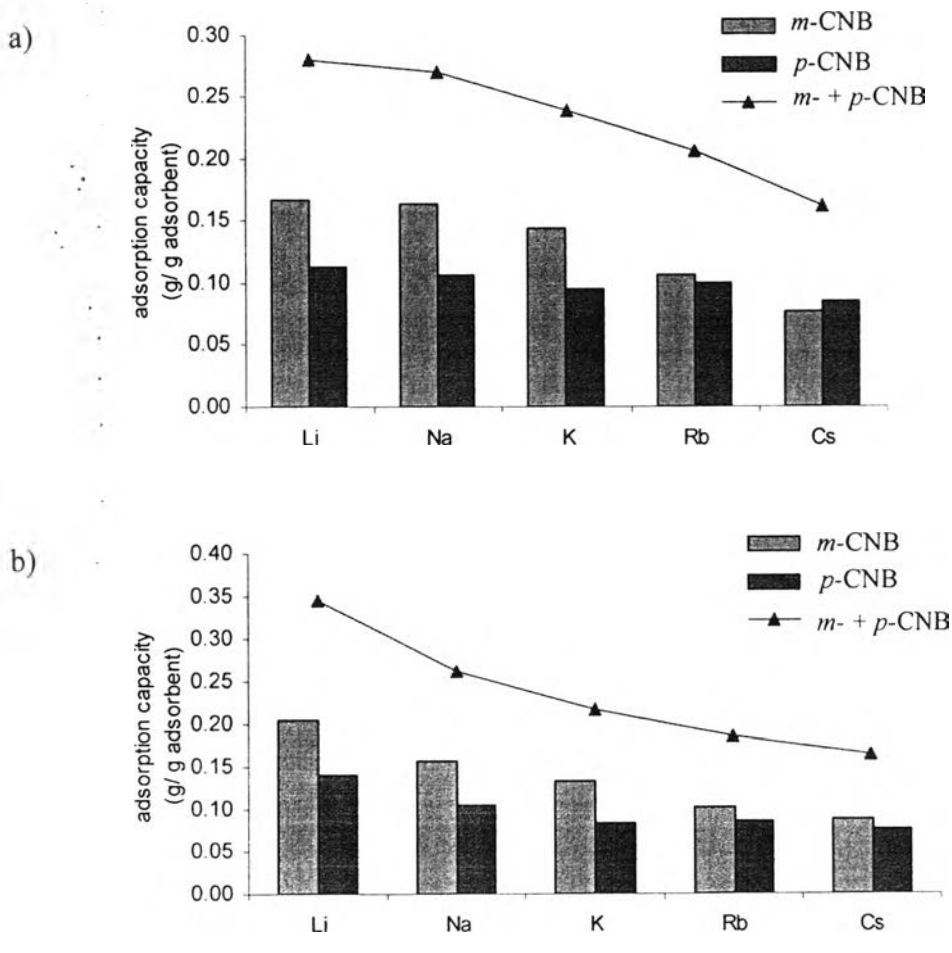

Figure 4.36 Competitive adsorption capacities as a function of cation exchanged zeolite a) Y zeolite b) X zeolite.

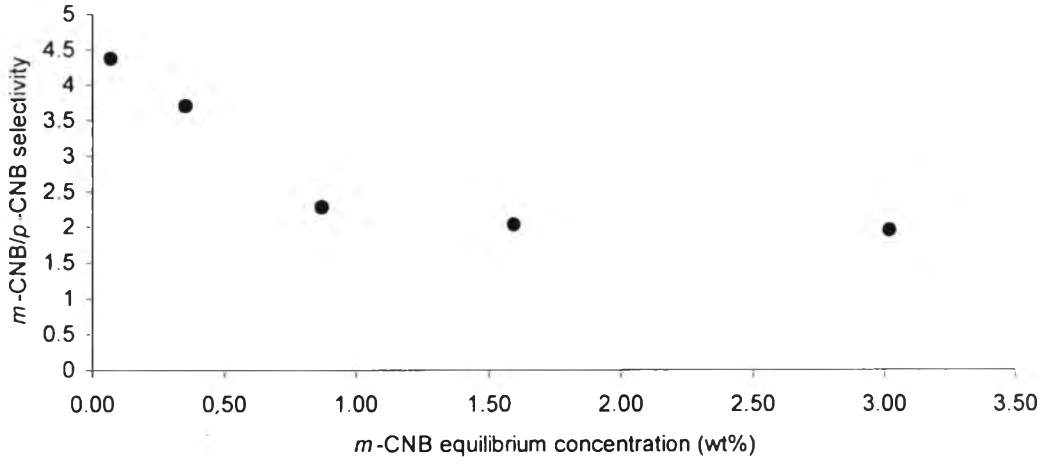

Figuren 4.37 *m*-CNB/*p*-CNB selectivity as a function of equilibrium concentration in liquid phase on NaY zeolite.

From Figure 4.37, the important thing in this curve is that the selectivity strongly depends on the composition in the fluid phase. The selectivity decreases with the increase in the liquid phase concentration. This behavior was previously reported by Rota *et al.* (1996). For a typical Langmuir adsorbed components, the selectivity should be constant and independent of the composition. Since selectivity is not constant, it is possible that the adsorbed phase may show a non-ideal behaviour (Titus *et al.*, 2003). At the low equilibrium concentration, the *m*-CNB/*p*-CNB selectivity is high or *m*-CNB is selectively adsorbed more than *p*-CNB. However, as the selectivity is calculated based on not only composition of adsorbates but also their counterparts in the fluid phase, even though they are comparable adsorption capacities for both *m*-CNB and *p*-CNB, the change in the compositions in the fluid is significant enough to increase the selectivity. After that the selectivity slightly decreases and remains relatively constant at the high equilibrium concentration. Even though, at the high equilibrium concentration (Figure 4.25), the *m*-CNB adsorption capacity is higher than that of *p*-CNB adsorption capacity, the *m*-CNB/*p*-CNB selectivity is low. That is because the *m*-CNB/*p*-CNB ratio in the fluid phase of the equilibrium solution is high.

To supports the previous hypothesis that the adsorption would preferentially take place on an adsorbent with higher acid strength than the lower one. The

correlation between the adsorption affinity of the CNBs and the strength of the adsorbent acidity was made. The Sanderson's intermediate electronegativity of the adsorbents (S_{int}) was calculated as a representative to the strength of the adsorbent acidity. The calculated S_{int} of the employed adsorbents are listed in Table A2. The higher S_{int} indicates high electron accepting ability and strong adsorbent acid strength (Kraikul *et al.*, 2006).

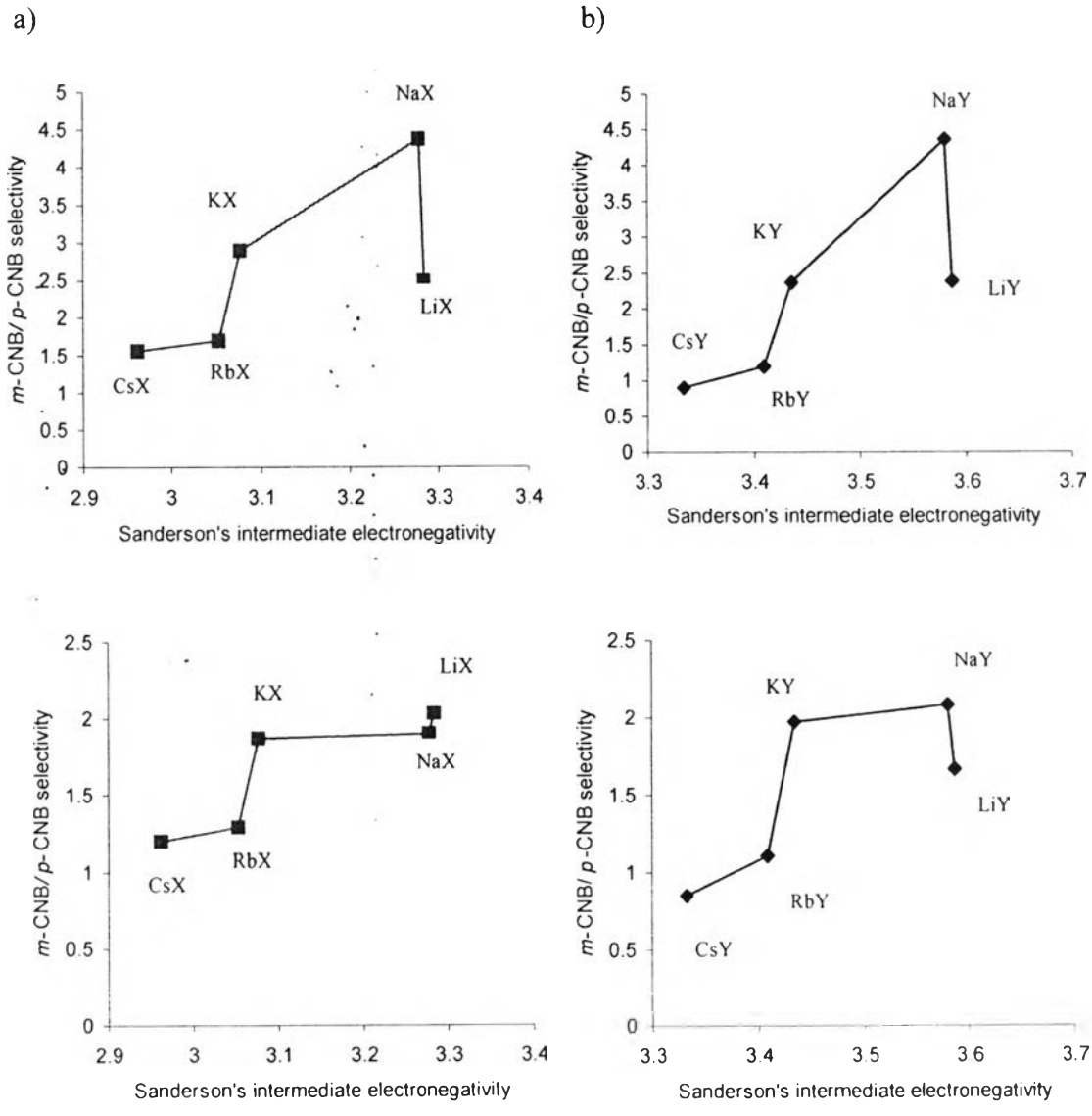

Figure 4.38 *m*-CNB/*p*-CNB selectivity at low (a and b) and high (c and d) equilibrium concentration as a function of Sanderson's intermediate electronegativity (S_{int}) for the various zeolites.

On the series of X and Y zeolites (Figure 4.38), the *m*-CNB/*p*-CNB selectivity over the alkaline exchanged X and Y zeolites increases as the strength of the zeolite acid strength increases. However, the selectivity decreases for LiY zeolite at the low concentration, and LiX and LiY zeolites at the high concentration even they have higher acid strength and contain a smaller cation size. As Li ions are located on S_I and S_{II} (Figure 4.23), distances between Li ions and adsorbates are large (Frising *et al.*, 2008). So, the interaction between the adsorbates and Li ions is lower and accessibility of adsorbate molecules to the adsorption sites is harder. Hence, the *m*-CNB/*p*-CNB selectivity decreases.

Even though the *m*-CNB capacities of LiX and LiY zeolites are the highest for both zeolites (Figure 4.36), the important factor to choose an appropriate zeolite to separate the isomers is selectivity. The *m*-CNB/*p*-CNB selectivities of NaY zeolite are the highest at low and high equilibrium concentrations. A reason that selectivities at low and high equilibrium concentrations must be considered is due to the use in a continuous process: the low concentration study (pulse test) and high concentration study (breakthrough test). Not only does NaY zeolite have the highest *m*-CNB/*p*-CNB selectivity in all cases, the adsorption capacities of both isomers on NaY zeolite are comparable to those of NaX zeolite. So the appropriate adsorbent for study is NaY.

4.3 Effect of desorbent

A desorbent liquid should be selected to have a boiling point significantly different from those of the feed components. In addition, the desorbent must be capable of displacing the feed components from the pores of the adsorbent. Conversely, it must also be possible for the feed components to displace the desorbent from the pores of the adsorbent. Thus, the desorbent must be chosen so as to be able to compete with the feed components for any available active pore space in the solid adsorbent, solely on the basis of concentration gradients (Sorbex Process, UOP).

X and Y zeolites are hydrophilic. The adsorbent is desorbed with an alkyl-substituted aromatic desorbent, which has different polarity, such as benzene, toluene etc. To study the desorbent-adsorbate interaction in a single component system and

the adsorbate-adsorbent and desorbent-adsorbent interaction in a multi-component system, five desorbents are chosen: benzene, toluene, *o*-xylene, *o*-dichlorobenzene, and nitrobenzene.

4.3.1 Single component adsorption

Single component adsorption isotherms for desorbents on NaY zeolite obtained at 30°C are shown in Figures 4.39 to 4.43. The adsorption capacities of the desorbents increase at the low concentration and reach the plateau region at the high concentration. With the increase in the adsorption amount, the affinity between the desorbent and the adsorbent decreases resulted from the shield against the adsorption sites (Liu, 2007). All adsorbents show the same trend of the adsorption isotherm. The adsorption isotherms are described by the classical Langmuir model.

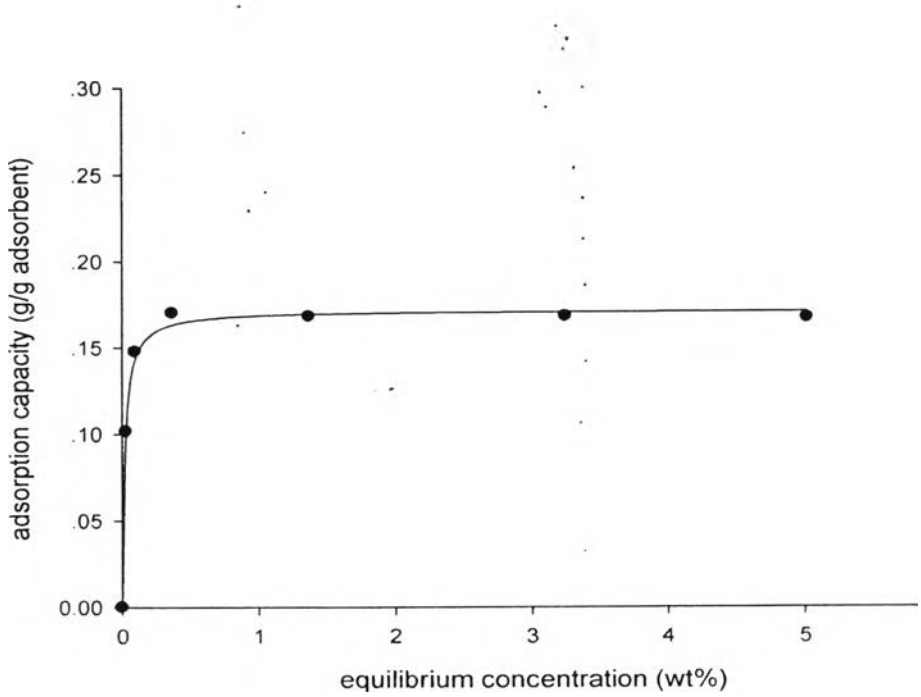

Figure 4.39 Adsorption isotherm for benzene on NaY zeolite at 30°C.

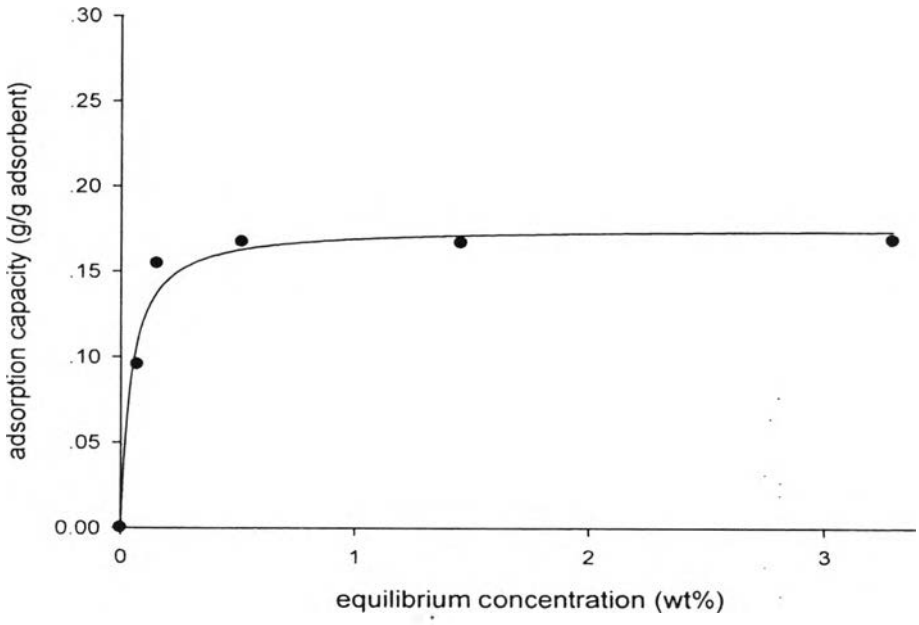

Figure 4.40 Adsorption isotherm for toluene on NaY zeolite at 30°C.

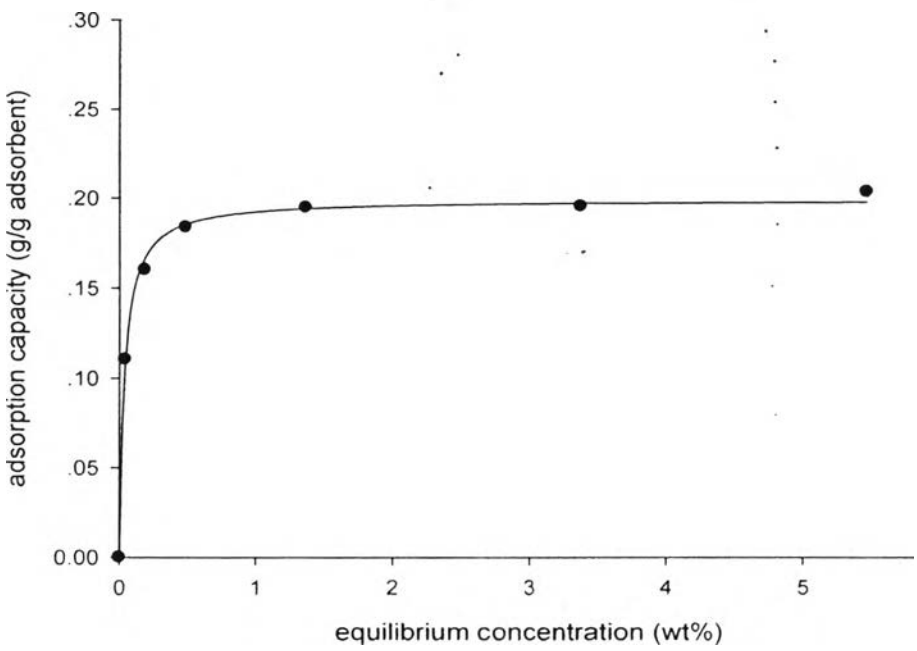

Figure 4.41 Adsorption isotherm for *o*-xylene on NaY zeolite at 30°C.

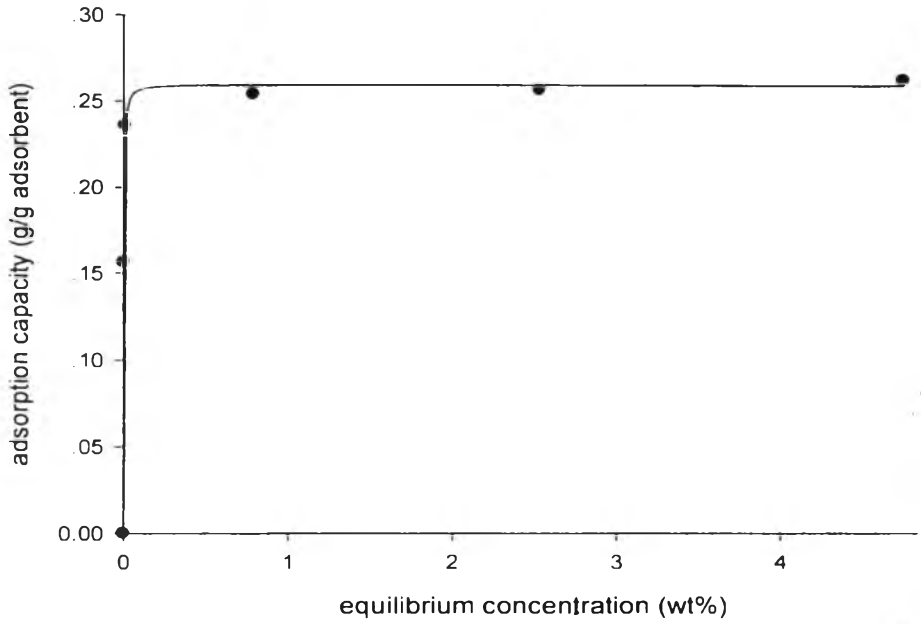

Figure 4.42 Adsorption isotherm for nitrobenzene on NaY zeolite at 30°C.

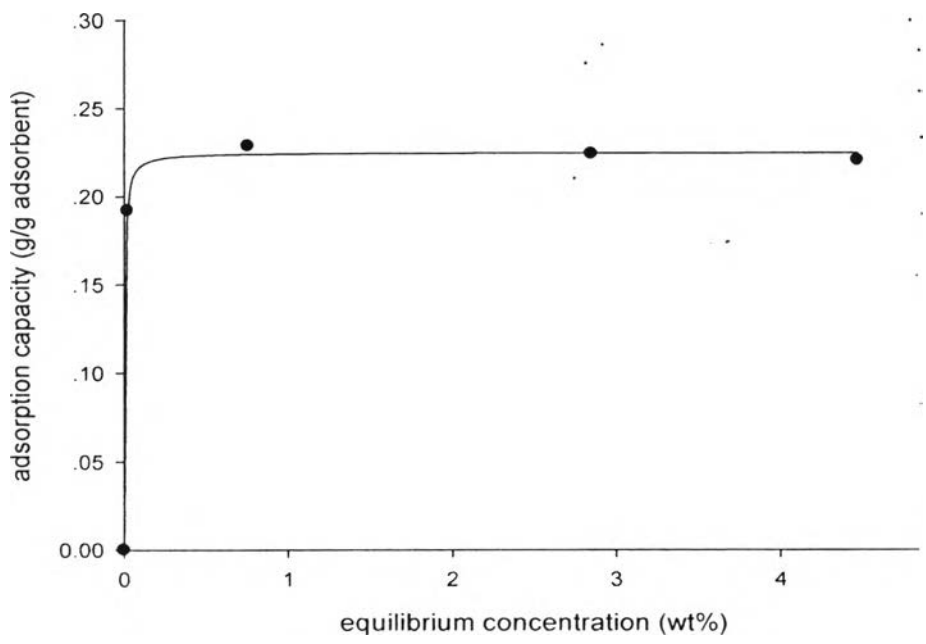

Figure 4.43 Adsorption isotherm for *o*-dichlorobenzene on NaY zeolite at 30°C.

The estimated values of the adjustable parameters of the isotherms, which are maximum capacity, equilibrium constant, and the coefficient of determination, R^2, are reported in Table B3. The R^2 values close to one indicate that the equa-

tion is a good description of the relation between the independent and dependent variables. The Langmuir model is fitted well with all experimental data. From Figure 4.44, the adsorption capacities of each compound are lower than that of *m*-CNB and *p*-CNB. This implies that the affinity of these compounds with the adsorbent is lower than that with *m*-CNB and *p*-CNB.

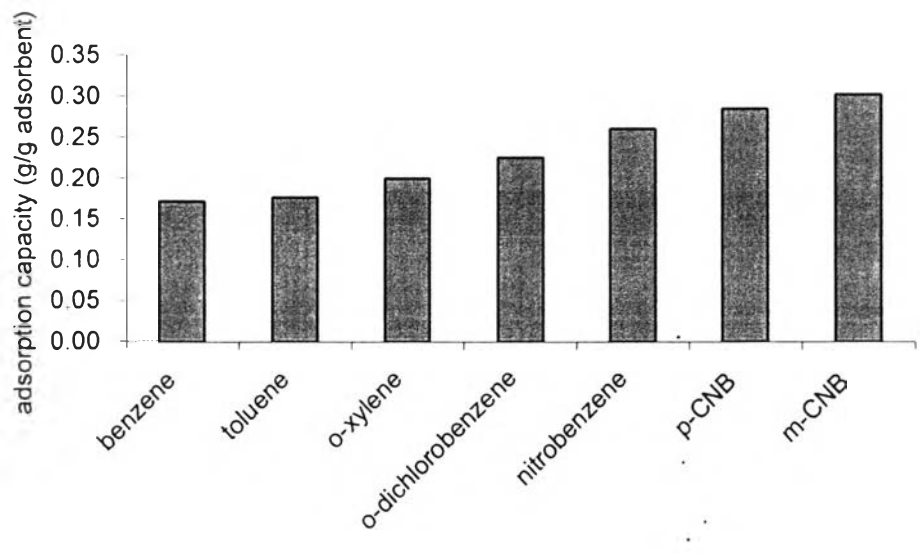

Figure 4.44 Adsorption capacity for each solvents on NaY zeolite at 30°C.

Benzene, toluene, and *o*-xylene are electron donating alkyl group that destabilizes the resonance structure in benzene ring. From their kinetic diameters (Table 4.2), benzene, toluene and *o*-xylene can pass through the NaY zeolite pore (7.4 Å). The adsorption capacity follows the order of *o*-xylene > toluene > benzene which follows the increase in the basicity. NaY zeolite with high acidity tends to adsorb the most basicity desorbent, *o*-xylene. Basicity of the desorbents increases when the benzene ring has alkyl group substituents (Olah, 1971).

Table 4.2 Desorbents with their dipole moments, molecular sizes and relative basicity to benzene

Desorbent	Dipole moment (*D*)	Kinetic diameter (Å)	Relative basicity to benzene
Benzene	0	5.27	1
Toluene	0.36	5.27	1.5
o-Xylene	0.62	5.6	1.8
o-Dichlorobenzene	2.27	-	-
Nitrobenzene	3.98	-	-

o-Dichlorobenzene and nitrobenzene are electron withdrawing groups that stabilize the docalized negative charge. Halogens and nitro groups substituents affect delocalized electron on the benzene ring by both inductive and resonance effect. When electrons on the benzene ring are withdrawn by nitro and chloro groups, it affects the electron density on the benzene ring. By considering the molecular dipole moment, nitrobenzene has higher molecular dipole moment. So it adsorbs on NaY zeolite more than *o*-dichlorobenzene. Although *m*-CNB and *p*-CNB have lower molecular dipole moments than nitrobenzene, their capacities are higher than that of nitrobenzene. A possible reason is that *m*-CNB and *p*-CNB have both halogen and nitro group and each group can interact with adsorption sites stronger than the one with only one substitute group.

4.3.2 Multi-component adsorption

The adsorption of the CNB isomers was carried out with NaY zeolite. Five solvents were now used as desorbents for the separation with n-dodecane as a tracer. The solvents are used for coadsorption in the system to consider the adsorbate-adsorbent and desorbent-adsorbent interaction.

Under acidic and basic adsorption sites in the FAU zeolite structure, the adsorption is believed to proceed via the specific interactions of ¶ electrons with

cations and CH with oxygens framework (Barthomeuf, 1996). The location of one aromatic in the zeolite depends on the balance between the adsorption on each site. In other words, the acidobasicity of an adsorbent determines the adsorptivity of an aromatic.

The strength of the desorbent represents the selectivity for *m*-CNB over a certain desorbent on the adsorbent. The factor represents the ratio of the adsorption strength of the adsorbent for the *m*-CNB to that of the desorbent. Too low a value of the factor indicates that the adsorption of the desorbent is very strong on the adsorbent, with the result that both *m*-CNB and other isomers of CNB will be eluted at close time. On the other hand, if the value of the factor is high, too much of the desorbent should be used for recovering all of the *m*-CNB (Guo and Long, 2001).

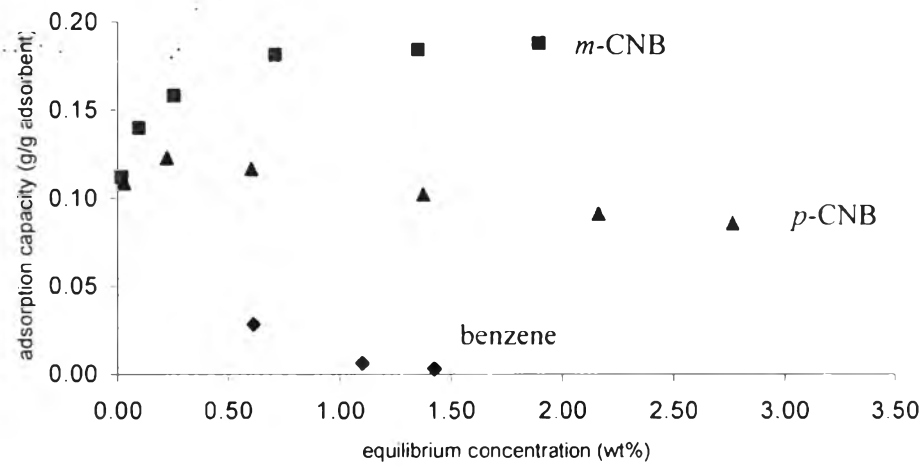

Figure 4.45 Competitive adsorption isotherms for *m*-CNB/*p*-CNB/benzene on NaY zeolite at 30°C.

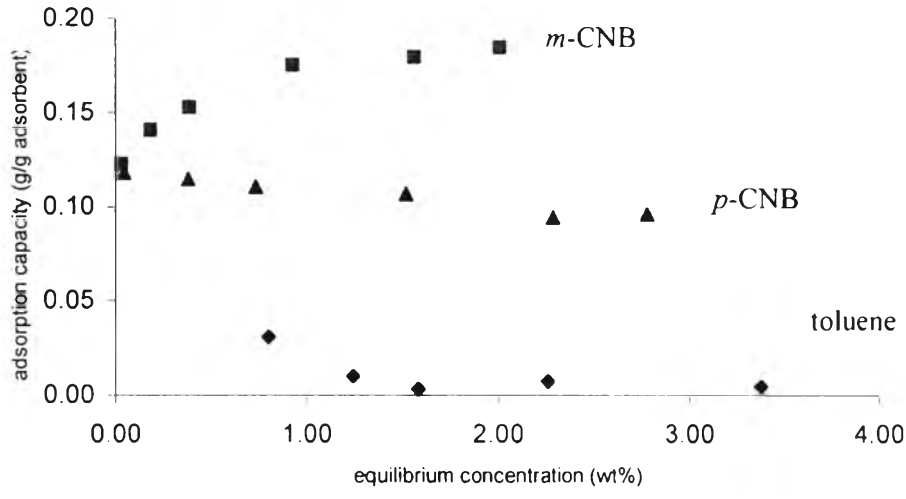

Figure 4.46 Competitive adsorption isotherms for *m*-CNB/*p*-CNB/toluene on NaY zeolite at 30°C.

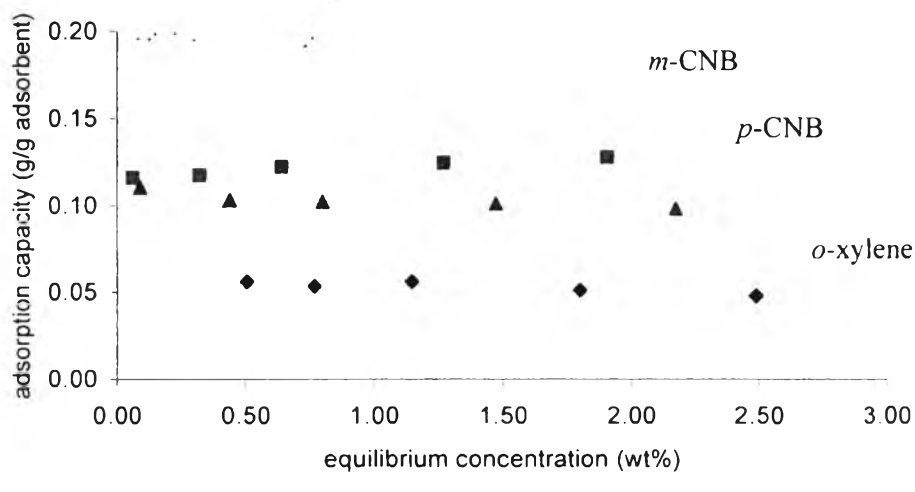

Figure 4.47 Competitive adsorption isotherms for *m*-CNB/*p*-CNB/*o*-xylene on NaY zeolite at 30°C.

From Figures 4.45 and 4.46, at the low concentration, there is enough space in the zeolite to receive all the species of the adsorbates. Therefore, *m*-CNB and *p*-CNB have the equal chance to reach the adsorption sites. The adsorption capacity follows the order of *m*-CNB > *p*-CNB > benzene and toluene. The *m*-CNB/toluene and *m*-CNB/benzene selectivities are infinite (Table 4.3), as both benzene and toluene have low electron density and hardly adsorb on the zeolite. Comparison be-

tween the *m*-CNB/*p*-CNB selectivities with and without a desorbent (Figure 4.38(d) and Table 4.3), those at the high concentration are 3.1 and 2.6 for the benzene and toluene systems, respectively, while that without a desorbent is 2.08. Even benzene and toluene do not adsorb on the zeolite, they interfere the adsorbate-adsorbent interaction.

Table 4.3 Selectivity of *m*-CNB relative to desorbents and *m*-CNB/*p*-CNB

Desorbent	Selectivity	
	m-CNB/desorbent	*m*-CNB/*p*-CNB
benzene	∞	3.11
toluene	∞	2.60
o-xylene	3.83	1.60
o-dichlorobenzene	0.21	0.64
nitrobenzene	0.59	4.13

For the *o*-xylene system in Figure 4.47, the adsorption capacity follows the order of *m*-CNB > *p*-CNB > *o*-xylene. The *m*-CNB/*o*-xylene selectivity is 3.83. This shows that the interaction of *o*-xylene to the zeolite is weaker than *m*-CNB and *p*-CNB. It means that the interaction of desorbent-adsorbent is not strong enough to displace the feed components from the pores of the adsorbent. The *m*-CNB/*p*-CNB selectivity is 1.6 and lower than that without a desorbent. *o*-Xylene may interfere the interaction of *m*-CNB and *p*-CNB.

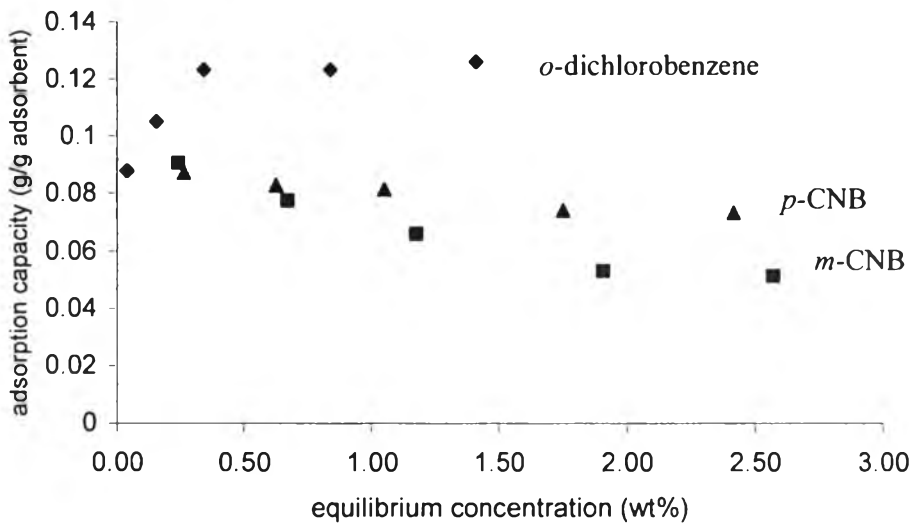

Figure 4.48 Competitive adsorption isotherms for *m*-CNB/*p*-CNB/*o*-dichlorobenzene on NaY zeolite at 30°C.

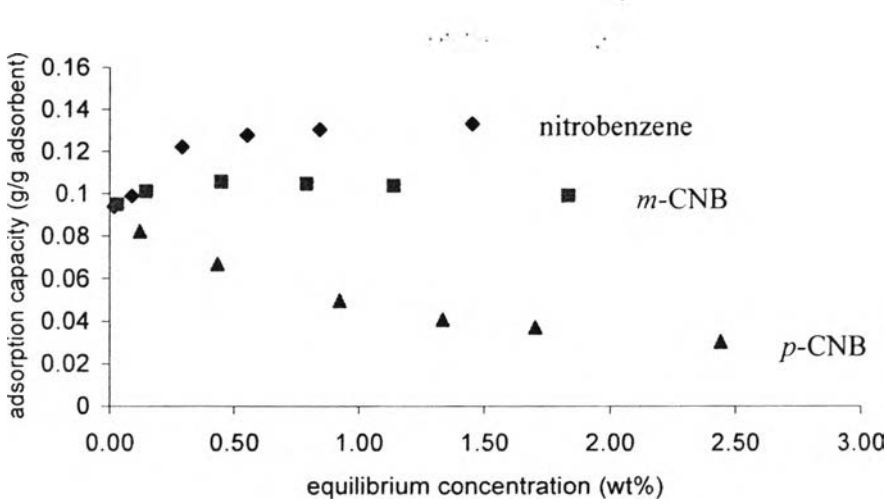

Figure 4.49 Competitive adsorption isotherms for *m*-CNB/*p*-CNB/nitrobenzene on NaY zeolite at 30°C.

o-Dichlorobenzene and nitrobenzene structures are similar to those of *m*-CNB and *p*-CNB. The adsorption capacity follows the order of *o*-dichlorobenzene > *p*-CNB > *m*-CNB (Figure 4.48). From Figures 4.45 to 4.47, adsorption capacities of desorbents increase with the increase in the molecular dipole moment of desorbents. But *m*-CNB adsorption capacities decrease due to competitive adsorption between desorbent and adsorbate to the adsorption sites. *p*-CNB adsorption capacities

are relatively constant. Desorbent affects *m*-CNB adsorption capacity than that of *p*-CNB. But the *o*-dichlorobenzene system, the *m*-CNB adsorption capacity is lower than that of *p*-CNB. The *m*-CNB/*o*-dichlorobenzene selectivity is 0.21. The desorbent is capable to displace the feed components from the pores of the adsorbent. However, the adsorption of the desorbent is very strong on the adsorbent due to the high dipole moment. With the low *m*-CNB/*p*-CNB selectivity, both *m*-CNB and *p*-CNB will likely be eluted at about the same time.

For the nitrobenzene system (Figure 4.49), the adsorption capacity follows the order of nitrobenzene > *m*-CNB > *p*-CNB. Comparison between Figures 4.48 and 4.49 shows that the adsorption capacity of nitrobenzene is higher than that of *o*-dichlorobenzene due to higher molecular dipole moments of nitrobenzene. The *m*-CNB/nitrobenzene selectivity is relatively constant at 0.59. And the *m*-CNB/*p*-CNB selectivity is 4.13 (Figure 4.50). The *m*-CNB/*p*-CNB selectivity from the binary competitive adsorption isotherm without a desorbent decreases as the *m*-CNB equilibrium concentration increases (Figure 4.37). The *m*-CNB/*p*-CNB selectivity with a desorbent is relative constant because of the desorbent-adsorbent interaction.

The best separation among the CNBs isomer is observed with the nitrobenzene system. It suggests that the balance between the adsorbent-adsorbates and adsorbent-desorbent interactions would be the best among all desorbents.

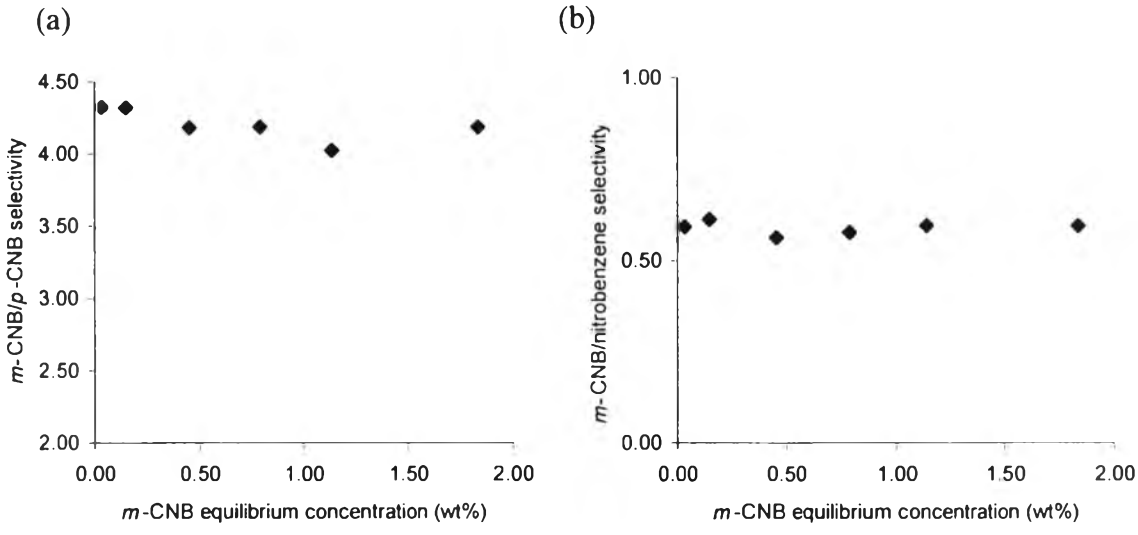

Figure 4.50 Selectivity from adsorption isotherms for *m*-CNB/*p*-CNB/nitrobenzene on NaY zeolite at 30°C (a) *m*-CNB/nitrobenzene selectivity and (b) *m*-CNB/*p*-CNB selectivity.

4.4 Effect of water content in zeolite

Physico-chemical properties of zeolites have been known to depend significantly on the number of Al atoms in their framework. The pairwise distribution of negative framework and positive cations induces a strong electrostatic field on the zeolite surface, which affects interaction energies with polar adsorbates (Kawai, 1992). Water molecules adsorb on zeolite surface through dipole-field interaction as well as hydrogen bonds with residual hydroxyl groups. Therefore, the affinity of zeolites with water molecules is dependent on their Si/Al ratio.

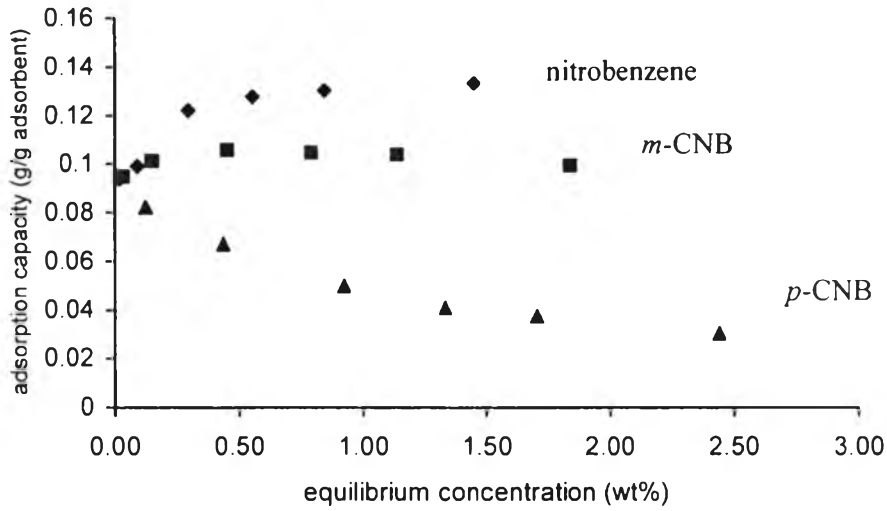

Figure 4.51 Competitive adsorption isotherms for *m*-CNB/*p*-CNB/nitrobenzene on NaY zeolite at 30°C and 4.09% LOI.

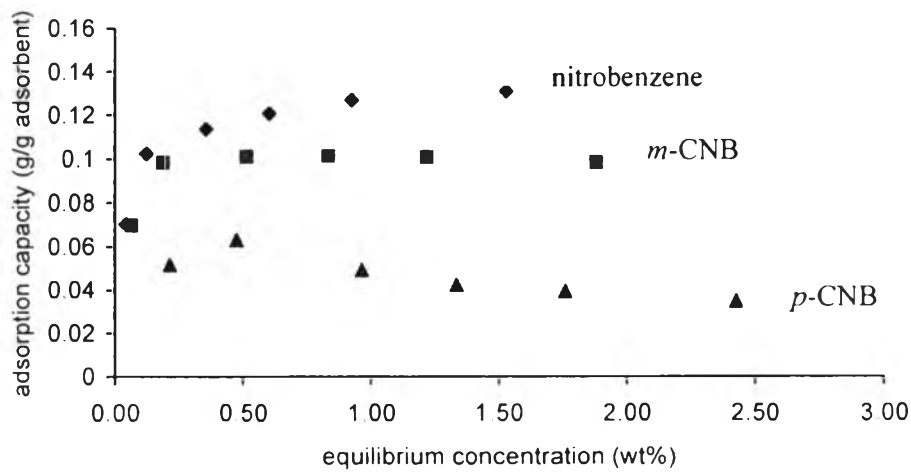

Figure 4.52 Competitive adsorption isotherms for *m*-CNB/*p*-CNB/nitrobenzene on NaY zeolite at 30°C and 5.05% LOI.

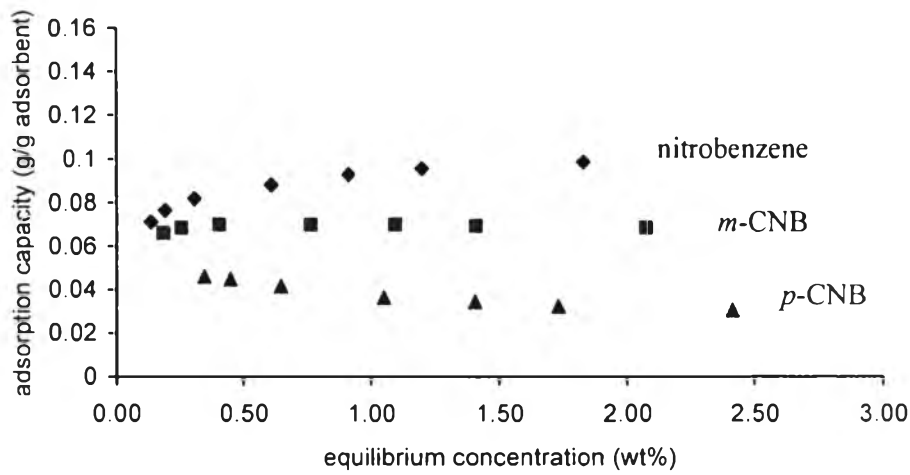

Figure 4.53 Competitive adsorption isotherms for *m*-CNB/*p*-CNB/nitrobenzene on NaY zeolite at 30°C and 9.82% LOI.

From Figures 4.51 to 4.53, the adsorption isotherms of *m*-CNB, *p*-CNB and nitrobenzene have the same trend with the increase in the water content but there are different in the total adsorption capacity. The nitrobenzene and *m*-CNB adsorption capacities decrease with the increase in the water content while the *p*-CNB adsorption capacity remains constant. So, the water content hardly affects the *p*-CNB adsorption capacity. From Table 4.4, total adsorption capacity decreases 27% when the water content in the zeolite structure increases from 4.09% to 9.82% LOI. That may be because the water molecule binds with the adsorption sites and blocks the desire adsorbed isomer. When the water content of zeolite increases, it has an influence on the adsorption behavior of the adsorbent due to the interaction between electrostatic field of zeolite surface and water dipole (Kawai, 1992).

Table 4.4 Influence of water content to the adsorption capacity and selectivity

Total water content (wt%)	*m*-CNB/nitrobenzene selectivity	*m*-CNB/*p*-CNB selectivity	Adsorption capacity (g/g adsorbent)			
			Nitrobenzene	*m*-CNB	*p*-CNB	Total
4.09	0.588	4.13	0.141	0.099	0.030	0.270
5.05	0.623	3.55	0.131	0.098	0.035	0.264
9.82	0.622	2.54	0.098	0.068	0.031	0.197

From Table 4.4, the *m*-CNB/nitrobenzene selectivity slightly increases and is almost constant at the high water content. Even though the water loading does not have the significant effect on the *m*-CNB/nitrobenzene selectivity when the water content is higher than 5.05% LOI, it affects the adsorption capacities of *m*-CNB and nitrobenzene. The *m*-CNB/*p*-CNB selectivity declines with an increase in the water co-ntent despite the fact that the *p*-CNB adsorption capacity is almost the same. The *m*-CNB/*p*-CNB separation is greatly affected by the moisture in the adsorbent.